Available online at www.sciencedirect.com
ScienceDirect
Sensors and Actuators B 121 (2007) 295–329
SENSORS AND ACTUATORS B CHEMICAL
www.elsevier.com/locate/snb

Electronic interfaces

Christian Falconi [a,*], Eugenio Martinelli [a], Corrado Di Natale [a], Arnaldo D'Amico [a,b,c], Franco Maloberti [d], Piero Malcovati [e], Andrea Baschirotto [f], Vincenzo Stornelli [g], Giuseppe Ferri [g]

[a] *Department of Electronics, University of Tor Vergata, Via Politecnico 1, 00133 Rome, Italy*
[b] *CNR IMM, Via Fosso del Cavaliere, 100, 00133 Rome, Italy*
[c] *CNR IDAC, Via Fosso del Cavaliere, 100, 00133 Rome, Italy*
[d] *Department of Electronics, University of Pavia Via Ferrata 1, 27100 Pavia, Italy*
[e] *Department of Electrical Engineering, University of Pavia Via Ferrata 1, 27100 Pavia, Italy*
[f] *Department of Innovation Engineering, University of Lecce, Via per Monteroni, 73100 Lecce, Italy*
[g] *Department of Electric Engineering, University of L'Aquila, Monteluco di Roio, L'Aquila, Italy*

Available online 13 November 2006

Abstract

Systems designed by humans have no "intelligence" and only execute algorithms; however, they may, somehow, mimic an intelligent behaviour (smart systems). Since, at present, information management in the electrical energy domain is extremely advantageous, smart systems require, all together, sensors, actuators, and electronic interfaces.

In literature there is some confusion, and even some contradiction, between the parameters used for characterizing the properties of sensors and of electronic interfaces. In the first part of the paper we provide a unified, coherent set of definitions which may be applied to both sensors and electronic interfaces. Afterwards we show how non-electrical systems may be conveniently analysed in the electrical domain by means of equivalent circuits, and we review some techniques for the design of high performance electronic interfaces; finally, we show a few examples, which illustrate the use of those techniques in practical applications.

Keywords: Electronic interfaces; Smart systems

1. Introduction

The interaction between living beings and the environment requires senses, decisions, and actions. Senses are necessary for gathering data from the environment; based on these data, living beings can take proper decisions in an "intelligent" way and, eventually, act on the environment. Humans have designed smart systems (see later) which use electronic systems, solid state sensors and actuators for mimicking an intelligent behaviour; these smart systems may significantly improve the quality of life, safety and health of humans; as a few examples, potential applications include more accurate diagnoses and more effective medical therapies, the reduction of repetitive work, the control of the environment, etc.

Any type of sensing or actuation mechanism has its limits. In some cases solid state sensors and actuators may largely exceed the performance of human senses and action capabilities (e.g. the bandwidth of the human ear is far more limited than the bandwidth of correspondent artificial systems). In other cases humans are much more evolved (e.g. robots may not walk as a human). In all cases, humans have intelligence, while smart systems can only execute algorithms; this fact is likely to remain unchanged for ever. Nevertheless, recent progresses in physics, chemistry, electronics, material science, bottom/up and top/down technologies made it possible to integrate high performance and low cost smart systems for a variety of applications (for instance, see [1–20]). As an example, a large array of nanodevices may constitute a macrodevice with very different properties in comparison with classic macrodevices; for instance, let us consider a classic loud speaker and an array of very small loud speakers which, globally, have the same output power as the classic system; clearly, the second system can operate at much higher frequencies in comparison with the classic one. This strategy

* Corresponding author.
E-mail addresses: falconi@eln.uniroma2.it, christian.falconi@gatech.edu (C. Falconi), damico@eln.uniroma2.it (A. D'Amico).

0925-4005/$ – see front matter © 2006 Elsevier B.V. All rights reserved.
doi:10.1016/j.snb.2006.09.022

is, in fact, already present in many biological systems such as the eye; the single receptor in the eye is sufficiently small for achieving a resolution of ½ square centimetre at about 10 m; however a single receptor would be useless (the field of view would be too limited), and therefore the eye contains millions of such very small receptors. As another example, nanotechnology opens the way to a new generation of nanosized transducers with an enormous potential for in vivo biomedical applications [21–27]; for instance, the single crystal ZnO nanostructures reported in [24–26] may find use as wireless nanotransducers for hyperthermia and targeted drug delivery [27].

In this paper we review the fundamentals of electronic interfaces which are essential components of sensors and sensors systems.

2. Signals and systems

2.1. Signals and linear, time invariant systems (LTI systems)

Signals are physical, chemical, or biological quantities which evolve with time; for instance, the current through a resistor, the temperature of a chip, and the velocity of a car are signals.

Signals can be classified into six different energy domains [1]: electrical, thermal, mechanical, magnetic, radiant, and chemical.

Systems transform input signals into output signals; for instance, a temperature controlled oven is a system which transforms the input signal x (position of a knob) into the output signal y (internal temperature), according to a given transformation

$$T: \quad x(t) \rightarrow y(t) \tag{1}$$

For simplicity, we consider single input–single output systems; clearly, if necessary, the definitions given here may be extended to multiple input–multiple output systems. A system is causal if and only if the condition

$$x_1(t) = x_2(t), \quad \forall t \leq t_0 \tag{2}$$

implies

$$y_1(t) = T[x_1(t)] = y_2(t) = T[x_2(t)], \quad \forall t \leq t_0 \tag{3}$$

(equivalently, a system is causal if and only if the output signal before t_0 only depends on the input signal values before t_0).

A system is time invariant if and only if, for any given t_0 and for any input signal $x(t)$,

$$T[x(t)] = y(t) \Rightarrow T[x(t - t_0)] = y(t - t_0) \tag{4}$$

A system is linear if and only if, for any real numbers c_1 and c_2, and for any input signals $x_1(t)$ and $x_2(t)$,

$$T[c_1x_1(t) + c_2x_2(t)] = c_1T[x_1(t)] + c_2T[x_2(t)] \tag{5}$$

Every real (physical, chemical, biological, ...) system is causal as the effect follows its cause.

Real systems are time variant and non linear. For instance, a resistor may be regarded as a system which transforms an input signal (current) into an output signal (voltage); although we often describe a resistor by means of the time invariant, linear Ohm's law,

$$v = Ri \tag{6}$$

this description is only accurate within a limited range of the input signal values (beyond those limits significant non linear effects occur); moreover, for a real resistor, the resistance, R, changes with temperature, contamination, aging, ... (i.e. the system is time variant). Nevertheless, almost always, real systems are approximated by means of correspondent linear, time invariant systems; in fact, in most cases this representation is both acceptable (within predefined operative conditions and for the time intervals which are of interest) and extremely convenient, as *time invariant, linear systems* are much easier to be analyzed and designed.

2.2. Instantaneous systems; error, relative error, accuracy, precision, sensitivity, resolution, offset

A system is instantaneous if, at any given instant, t_0, the output of the system only depends on the input signal at the same instant, so that

$$y_{\text{out}} = f(x_{\text{in}}) \tag{7}$$

Instantaneous systems, by their definition, are time invariant (linear or non linear) systems.

In principle, no real system can be instantaneous; in fact, systems transform input signals into output signals, and, in the real world, signal transformations take time (i.e. are not instantaneous). However, time invariant systems which are "much faster than their input signals" may be considered as instantaneous (see later for a more quantitative definition); as we shall see, very important properties of measurement systems (and, in particular, of sensors and electronic interfaces) are defined under this assumption.

An ideal system transforms an input signal into an output signal according to a desired transformation; however, as shown in Fig. 1, a real system unavoidably introduces an error. In the case of instantaneous systems, the error may be defined as the difference between the output and the ideal output

$$e(x_{\text{in}}) = y_{\text{out}}(x_{\text{in}}) - y_{\text{out,ideal}}(x_{\text{in}}) \tag{8}$$

The error *depends* on the input; for instance, a system might have a very small error only when the input is within a certain range. For simplicity, we assume that: there is no error (or, in practice, a very small error) in the input signal; the ideal output

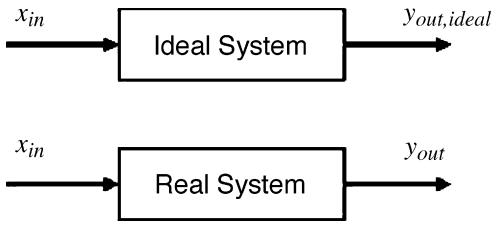

Fig. 1. Ideal system and real system.

is known without uncertainty; the output may be measured with negligible errors. The relative error, e_r, is defined as

$$e_r(x_{in}) = \frac{y_{out}(x_{in}) - y_{out,ideal}(x_{in})}{y_{out,ideal}(x_{in})} \quad (9)$$

Clearly, if the ideal output is zero, the relative error may not be defined; more in general, the relative error is only meaningful if

$$\{|y_{out}(x_{in}) - y_{out,ideal}(x_{in})| \ll |y_{out,ideal}(x_{in})|\} \Rightarrow |e_r(x_{in})| \ll 1 \quad (10)$$

The accuracy may be qualitatively defined as the capability of the system to produce small errors. The reported definitions of the error, the relative error, and the accuracy refer to a "single event"; however, if a number of events are considered, the output may be regarded as a random variable $Y_{out}(x_{in})$. Under the previously discussed assumptions (no error in the input, known ideal output, and output measured with negligible errors), the average error may be computed

$$e_{AVG}(x_{in}) = E[Y_{out}(x_{in})] - y_{out,ideal}(x_{in}) \quad (11)$$

where $E[Y_{out}]$ is the mean value of the random variable Y_{out}; clearly, the average error depends on the input. If we consider the accuracy as the capability of the system to produce small *average* errors, a system may be accurate even if the standard deviation of Y_{out} is very large; this would be unacceptable in many practical cases as a single measurement would not necessarily be accurate (while the average of many measurements, assuming a constant input, would be accurate). For this reason, it is important to specify the *precision* which is related to the standard deviation of the random variable Y_{out}. In order to intuitively illustrate these concepts, we may consider 10 events and the values reported in Fig. 2 for both the ideal output and the output y_{out} in correspondence of each event; a system may be: accurate and precise (system A); precise, but not accurate (system B); accurate, but not precise (system C, which has a small average error); neither accurate neither precise (system D).

The sensitivity of an instantaneous system is defined as

$$S = \left.\frac{\partial y_{out}}{\partial x_{in}}\right|_Q \quad (12)$$

and, in general, depends on the operating point Q. Clearly, the sensitivity is a pure number if and only if the input and the output signals are homogeneous; in this case, the sensitivity is also called *gain*, G (e.g. the sensitivity of a voltage amplifier is a gain, since both the input and the output signals are voltages). If the sensitivity is not a pure number, it may not be considered a *gain* and must be expressed with proper dimensional units (e.g. for a current to voltage converter, which has a current input and a voltage output, the sensitivity must be expressed in Ω). With reference to Fig. 3 [6], a smart system may comprise a direct chain (from the measurand, M, to the A/D conversion block) and other blocks including power management (energy block), the transducer/receiver block (T/R), a memory, a microcontroller and the actuators. The different types of sensitivities for such a system are listed in Table 1 (where both linear and non linear systems are considered). It is important to stress that the sensitivity may

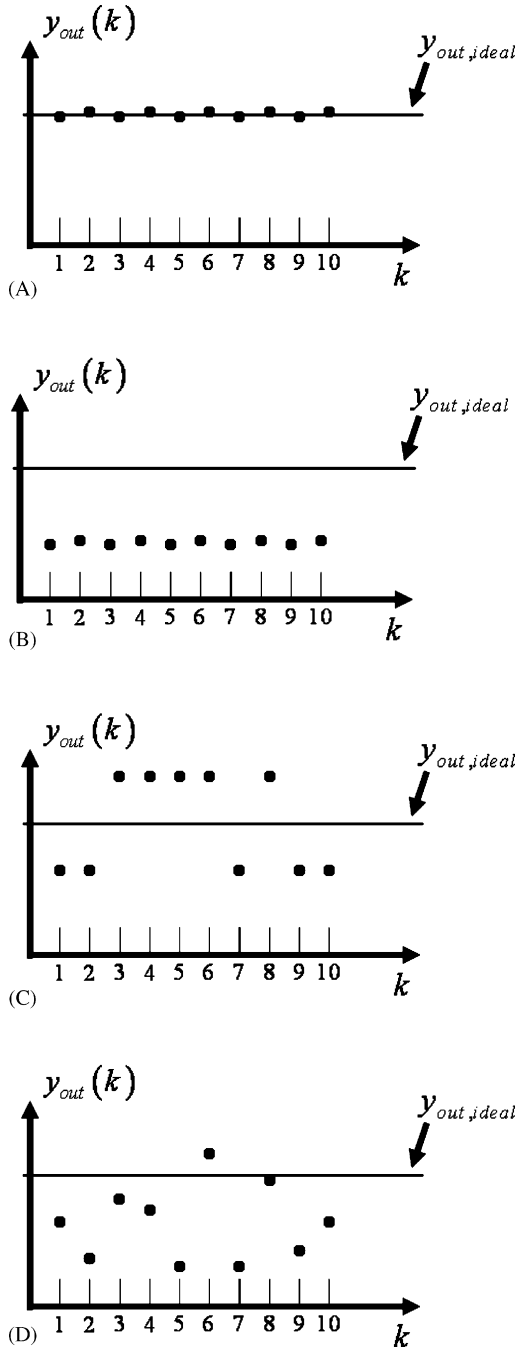

Fig. 2. Systems with different accuracy and precision.

only be defined for instantaneous system and, for instance, the "filter sensitivity" is *not* the transfer function of the filter and may only be defined if the filter is much faster than its input signals (i.e. it may be considered an instantaneous system, see later). The *output offset* y_{OFF} is defined as

$$y_{OFF} = f(0) \quad (13)$$

that is the output when the input signal is zero. The solutions of the equation

$$0 = f(x_{in}) \quad (14)$$

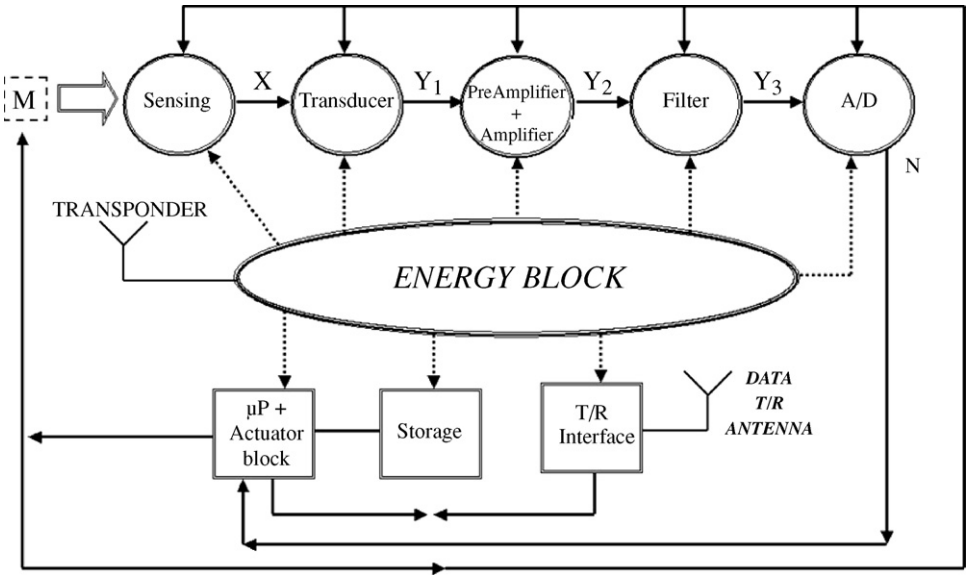

Fig. 3. Block scheme for a smart system.

are the *input offset* values; in principle, there might be no solution or many solutions for the Eq. (14); however, if the function f is monotonic, which is often the case, there may be no more than one *input offset* x_{OFF}.

In a given operating point, Q, there is a minimum variation of the output signal, Δy, that can be detected (this quantity may not be zero because of noise and interferences); the minimum variation of the input signal which may be detected is the resolution (relative to the operating point Q)

$$R = \Delta x = \frac{\Delta y}{S|_Q} = \frac{\Delta y}{(\partial y_{out}/\partial x_{in})|_Q} \tag{15}$$

If we now consider a linear, instantaneous (which is also, by definition, time invariant) system, we find

$$y_{out} = f(x_{in}) = Sx_{in} + y_{OFF} = S(x_{in} - x_{OFF}) \tag{16}$$

where the previous definitions of sensitivity, together with the *output offset* and *input offset* have been applied; clearly, the sensitivity of linear instantaneous systems is constant (and does not depend on the operating point) and the following relation between the *input offset*, the *output offset*, and the sensitivity applies

$$y_{OFF} = -Sx_{OFF} \tag{17}$$

Moreover, in the case of linear instantaneous systems we may apply the definition (8)

$$\begin{aligned} Y_{out,ideal} &= S_{ideal}x_{in} + Y_{OFF,ideal} = S_{ideal}(x_{in} - x_{OFF,ideal}), \\ Y_{out} &= Sx_{in} + Y_{OFF} = S(x_{in} - x_{OFF}), \\ e &= Y_{out} - Y_{out,ideal} \\ &= (S - S_{ideal})x_{in} + (y_{OFF} - y_{OFF,ideal}) \\ &= (S - S_{ideal})x_{in} + (S_{ideal}x_{OFF,ideal} - Sx_{OFF}) \end{aligned} \tag{18}$$

It is then evident that the error is constituted by a term which is proportional to the input signal and an offset error which does not depend on the input. It is useful to define both the sensitivity error S.E. and the relative sensitivity error R.S.E. as follows

$$\text{S.E.} = S - S_{ideal}, \qquad \text{R.S.E.} = \frac{S - S_{ideal}}{S_{ideal}} \tag{19}$$

As we discussed, if the input and the output signals are homogeneous, the sensitivity is also called *gain* and the following definitions for the gain error G.E. and the relative gain error R.G.E. apply

$$\text{G.E.} = G - G_{ideal}, \qquad \text{R.G.E.} = \frac{G - G_{ideal}}{G_{ideal}} \tag{20}$$

Table 1
Sensitivities in the smart system shown in Fig. 3

	Non linear response			Linear response			Linear response without offset			
${}^{I}S$	$\frac{\partial X}{\partial M}$			$\frac{\Delta X}{\Delta M}$			$\frac{X}{M}$			Internal sensitivity
${}^{T}S$	$\frac{\partial Y_1}{\partial X}$			$\frac{\Delta Y_1}{\Delta X}$			$\frac{Y_1}{X}$			Transduction sensitivity
${}^{A}S$	$\frac{\partial Y_2}{\partial Y_1}$			$\frac{\Delta Y_2}{\Delta Y_1}$			$\frac{Y_2}{Y_1}$			Analog amplification or transamplification
${}^{F}S$	$\frac{\partial Y_3}{\partial Y_2}$			$\frac{\Delta Y_3}{\Delta Y_2}$			$\frac{Y_3}{Y_2}$			Analog filter sensitivity
${}^{O}S$	$\frac{\partial Y_1}{\partial M}$,	$\frac{\partial Y_2}{\partial M}$,	$\frac{\partial Y_3}{\partial M}$	$\frac{\Delta Y_1}{\Delta M}$,	$\frac{\Delta Y_2}{\Delta M}$,	$\frac{\Delta Y_3}{\Delta M}$	$\frac{Y_1}{M}$,	$\frac{Y_2}{M}$,	$\frac{Y_3}{M}$	Global sensitivities

Finally, we remark that, in general, the error, the relative error, the accuracy, the precision, the sensitivity, and the resolution depend on the input; whether this dependence may or may not be neglected (so that the correspondent parameter may be approximated by a constant for a certain input values range) must be a matter of discussion in the sensor design phase.

2.3. Linear, time invariant systems; transfer functions

If a system is linear and time invariant, it can be completely described from the external point of view by its transfer function, which is the Fourier transform of its impulse response. In fact, if the system transfer function is known, for any given input signal $x_{in}(t)$, the output may be found as

$$y_{out}(t) = \Im^{-1}\{H(f)X_{in}(f)\} \quad (21)$$

where $\Im^{-1}$ denotes the inverse Fourier transform, while $H(f)$ and $X_{in}(f)$ are, respectively, the system transfer function and the Fourier transform of the input signal.

The transfer function of an instantaneous LTI system is a constant and is the sensitivity of the system (this is obvious from (16)). On the other hand, since instantaneous systems, strictly, may not exist because of the finite speed of real systems, transfer functions of real systems always depend on frequency; in practical cases, transfer functions may only be *approximately* constant (e.g. within 3 dB) within a certain range of frequencies, which is called the *bandwidth* (e.g. 3 dB bandwidth). All real systems have a limited speed and, therefore, have a finite bandwidth (because they may not respond to signals beyond certain frequencies); moreover, most measurement systems have a low pass behaviour; if the Fourier transforms of all possible input signals is practically zero outside the bandwidth of these low pass "filters", these systems may be considered instantaneous, or, equivalently, they are "much faster than their input signals".

3. Transducers, electronic interfaces, and smart systems

3.1. Transducers, sensors, and actuators

Transducers are systems which convert signals from one energy domain into signals in a different energy domain. Sensors may be defined as systems which convert signals in non-electrical domains into electrical signals; for instance, a temperature (thermal domain) to resistance (electrical domain) transducer is a sensor; actuators are the complementary class of systems which convert electrical signals into non-electrical signals; for instance, an (electrically driven) heater is an actuator.

We stress that there are different interpretations of the terms "transducers" and "sensors" [1–6]. For instance, "a sensor is often defined as a device that receives and responds to a signal" [2]; with this definition the word "sensor" would be synonymous of "system", which is coherent with the fact that a "sensitivity" may be defined for any (instantaneous) system; however, it is also possible to consider a sensor as "a device that receives a stimulus and responds with an electrical signal" [2]; in other references [1] the authors refer to "input transducers" instead of sensors. The reason for this apparent confusion lies in the broad definitions of "transducers" and "sensors". As an example, let us consider a temperature dependent resistor and an electronic interface which produces an output voltage related to the temperature dependent resistance; the temperature dependent resistor is both a sensor and a transducer; however, the complete system is also both a sensor and a transducer (as it transforms a temperature variation into a voltage variation); it is then possible to refer to the temperature dependent resistor as the transducer and to the complete system as a sensor (i.e. the sensor includes the transducer). In any case, these different definitions are seldom a problem, as the exact meaning of the words "sensor" and "transducer" is generally easily understandable from the context (for instance, in [18,19] it is obvious that the authors consider the electronic interface as a part of the sensor).

3.2. Smart systems and electronic interfaces

In contrast with living beings, systems designed by humans do not possess "intelligence" and can only execute algorithms; however, in many practical cases, these "non-intelligent" systems may, somehow, mimic an intelligent behaviour. As an example, almost every car nowadays contains systems which, whenever necessary, may activate safety devices such as air bags, anti-blocking systems, ... We refer to this type of non-intelligent systems which are designed by humans and, somehow, "seem" intelligent as "*smart systems*".

In order to "seem" intelligent, a smart system must invariably, first, acquire information on the environment, second, determine the appropriate action to be undertaken, and, third, act accordingly; this necessary process is, obviously, an imitation of the natural behaviour of living beings.

Smart systems manipulate signals belonging to different energy domains; however, when designing a smart system, there is almost no choice about the selection of the energy domains. In fact, in principle, the designer could only choose the energy domain in which the information may be processed as the other energy domains are implicitly specified by the definition of the system. A simple example easily illustrates this point; an automatic system for regulating the temperature of an object must measure its temperature (i.e. extract information from the environment), determine the proper action to be undertaken (i.e. heating or cooling), and act accordingly; the determination of the appropriate action corresponds to process the information (for instance, comparison between the measured temperature and the desired temperature). Obviously, the definition of the system automatically determines the energy domains of all the signals but those for processing the information (in our example, temperature is in the thermal energy domain). In principle, the information might be processed in any energy domain (e.g. it has even been argued [28] that signal processing in the mechanical domain could, some day, have some advantages); nevertheless, there is no doubt that, at present, the impressive progress of electronics (and, especially, of *digital* electronics) makes it extremely convenient to generate, elaborate, memorize, and transmit signals in the electrical domain (as an example, a

state of the art digital system can perform billions of operations per second in a reliable, accurate, low cost, and low power manner).

As a result, every smart system must bring the measured information from a non-electrical energy domain into the electrical domain (sensors), and bring the actuation decision from the electrical domain into a non-electrical energy domain (actuators). In practice, smart systems gather data on the environment through sensors, take proper decisions through electronic systems, and act through actuators. This is why sensors and actuators are so important in smart systems.

The sensor response (i.e. the output signal of the sensor) is analog because "the real world is analog"; since today it is extremely convenient to manipulate (generate, elaborate, memorize, transmit, etc.) information in the *digital* electrical domain, in order to include a sensor into a smart system, a circuit which transforms the sensor response into a digital signal is necessary. For instance, converting the resistance of a resistive sensor into a digital signal may be done by injecting a reference current into the resistor, amplifying the voltage across the resistor, and converting this voltage into a digital signal by means of an analog to digital converter (ADC). More in general, electronic interfaces are the circuits (including special functions, such as auto-calibration, sensor biasing, etc.) which convert the sensor responses into signals which are easy to be processed (i.e., almost always, voltage *digital* signals); strictly, electronic interfaces are also required for converting digital signals into proper signals for driving the actuators; however we shall focus on electronic interfaces for sensors as in most cases these are the critical part of a smart system. Electronic interfaces are essentially analog circuits which, almost invariably, include an analog to digital converter and, in some cases, also include some digital sub-systems.

The importance of electronic interfaces in smart systems may now be appreciated: sensors bring the measured information from a non-electrical energy domain into the electrical domain; however, in practice, it is convenient to process the acquired information with *digital* electronic systems and, therefore, a circuit (electronic interface) is required for converting the (electrical) sensor response into a convenient *digital* electrical signal; in the same manner, actuators require an electronic interface. The critical role of analog electronics in systems design (see, for instance, [29]) is largely due to the importance of electronic interfaces; in fact, depending on the application, it may be necessary that electronic interfaces meet stringent specifications for noise, voltage supply, power consumption, speed, interferences rejection, low cost, reliability, etc. Besides, the design of the electronic interface generally requires models for the transducers (for instance, it would not make sense to design an electronic interface which is much more accurate and faster than the transducer to be interfaced). In many practical cases, the design of high performance electronic interfaces is a main obstacle to the implementation of successful smart systems.

Strictly, within our definitions, electronic interfaces may be accurate, power efficient, low voltage, fast, but not "smart"; in the same manner, sensors may also be accurate, low cost, integrated, but not "smart". In fact, we have associated the word "smart" to systems which are designed by humans and "seem" intelligent; however, since a rigorous definition of what "seems" intelligent would also be problematic, it is appropriate to refer to smart systems whenever the sensors and the electronics might enable an easy implementation of smart systems (e.g. a system which contains both a temperature sensor and the interface in the same chip and provides a digital output deserves the attribute "smart" as it may be easily incorporated in a system which might "seem" intelligent).

4. Limits to the accuracy and precision of electronic interfaces

4.1. Time invariance and speed requirements for electronic interfaces

Although, strictly, real systems are time variant, in many practical cases the time invariance hypothesis is useful. Apparently, such hypothesis may be even more questionable for some sensors and electronic interfaces which, by definition, are time variant; as an example, a temperature resistive sensor is already a time variant system because its resistance changes with time (due to temperature variations). Depending on the application, this may or may not be an issue; for instance, if the variations of the temperature dependent resistance are very slow when compared with all other variations in the system, we may just consider a constant resistance and make sure that the complete system properly works with all the possible resistance values. We mention that this is not always a problem; as an example, the output signal of a thermocouple is a voltage and its variations do not imply variations of systems components (which would be a clear indication of time variance).

In most cases the performance of sensors and electronic interfaces are described by their error, relative error, accuracy, precision, sensitivity, resolution, and offset. Since these concepts are well defined only for instantaneous systems (which are a *sub-set* of time invariant systems), sensors and electronic interfaces must be much faster than their input signals. More in general, measuring means comparing the measurand with a reference quantity (which, ideally, is *constant*); clearly, the measurand should be *constant* during all the measurement process; in practice, the measurement process must be much faster than possible variations of the measurand. As an example, a temperature sensor has a resolution of 0.1 K if it is able to distinguish temperature variations as small as 0.1 K, *assuming that temperature variations* (i.e. the input signal of the sensor) *are much slower than the sensor*. In many (but not all) electronic interfaces, this is not a problem, because the input signals of electronic interfaces are typically much slower than electrical systems; as an example, in the design of a temperature sensor the bandwidth requirement for the electronic interface may be as low as 10 Hz because temperature variations are rather slow. As an important consequence, designers may conveniently trade accuracy for speed; this is definitely one of the keys for high accuracy electronic interfaces design (e.g. $\Sigma\Delta$ analog to digital converters are widely used in electronic interfaces [19,30–35]).

4.2. Accuracy and precision

As we have seen, instantaneous systems may be characterized by their error, relative error, accuracy, precision, sensitivity, resolution, and offset. These definitions may be used for any measurement system, as long as it may be considered instantaneous (i.e. much faster than its inputs); sensors and electronic interfaces, clearly, are a sub-set of measurement systems and, therefore, their performance should be expressed in the same manner. A rigorous use of the same definitions for both the sensors and the electronic interfaces is preferable, as it helps a clear understanding of the design challenges and opportunities (for instance, it would not make sense to waste resources for designing an interface which has an accuracy much higher than its sensor). Furthermore, the same definitions should be applied, whenever it is possible, to sub-systems of the electronic interface. For instance, a voltage amplifier which has a negligible input offset voltage and a very small relative gain error, has an high accuracy; however, if that amplifier has a significant input equivalent noise (with zero mean value), its precision could be poor; clearly, if such an amplifier is inserted in the measurement chain, the precision of the electronic interface (and, hence, of the measurement system) could be poor as well. It is therefore advisable to characterize the sensors, the electronic interface and its sub-systems with the same set of definitions (on the contrary it is very common in literature to refer to "high precision" circuits instead of "high accuracy and high precision", and so on).

If the error must be small for every measurement, we need an accurate and precise electronic interface; if only the mean value of the error (with reference to many measurements) is important, an accurate system is sufficient.

Depending on the application, electronic interfaces must meet stringent specifications for noise, minimum supply voltage, power consumption, speed, interferences rejection, low cost, reliability, ... These specifications may be translated into accuracy and precision requirements; for instance, saying that the power consumption must be below 1 mW, we mean that the required accuracy and precision must be obtained with an interface which has a power consumption below 1 mW. It is instructive to consider some sources of errors in a measurement.

Measuring is comparing a measurand with a reference quantity; the reference quantity is a *constant* which is "real" (e.g. the resistance of a reference resistor) or may be indirectly deduced from different signals (e.g. a reference resistance may be deduced from an equivalent switched capacitor circuit with resistance $R = 1/fC$). The accuracy and precision of a measurement may not be better than those of the reference quantity; this is why high performance references are very important. In some cases, high quality references are available; in other cases, the reference signal must be generated by the interface itself (for instance, voltage references are essential building blocks for many electronic interfaces, so that the design of accurate and precise integrated bandgap references is a main issue [36–42]).

Beside the errors of the reference, errors also occur in the comparison process; the errors of analog digital converters, for instance, fall in this class of errors.

Additionally, the perturbation which is necessarily introduced by any measurement action should be negligible for the desired level of accuracy. Electronic interfaces must measure electrical variations without significantly perturbing the transducer under test; as an example, impedance loading effects must always be evaluated; as another example, interfaces for temperature resistive sensors should avoid significant self heating errors.

5. Equivalent electric circuits

In most practical cases simulation is necessary for the accurate analysis of analog circuits. In fact, the extremely complex models of electronic devices [43–45] (e.g. MOSFETs fabricated with deep submicron CMOS processes) make it almost impossible to achieve an accurate, theoretical analysis of even the simplest analog circuits.

On the other hand, simulators, by themselves, are not able to design even the simplest analog circuits. In fact, the number of circuits that can be made of even a few transistors is exceedingly too large to be systematically analysed by simulators; this is why, in spite of many attempts, *automatic* design of analog circuits is still not possible (and, in the opinion of most analog designers, will never be possible; interestingly, *automatic* design of digital systems is highly effective).

This is, in particular, true for electronic interfaces (i.e. a class of analog circuits): simulators are not able to design even the simplest interface, but their judicious use constitutes an invaluable tool. There is, however, an additional challenge: although, by definition, electronic interfaces are just electronic circuits, their design generally requires an accurate model of the sensors, independently on its complexity. In some cases, the transducers are just electronic devices; even in these cases, models which are satisfactory for most electronic designs may be not enough accurate for the design of high performance electronic interfaces and sensors (see, for instance, [16,46–48] for the problem of accurately modelling bipolar transistor as thermal sensors). In other cases, transducers are non-electrical and it may be non obvious how to simulate these transducers together with the rest of the electronic interface. Almost always, the best practical solution is to model non-electrical signals and systems by means of *equivalent* signals and systems in the electrical energy domain, so that the complete system may be analyzed by means of standard simulators for electronic circuits such as SPICE. Obviously, one could conceive a dual approach, that is modelling electrical signals and systems by means of *equivalent* signals and systems in different energy domains; in practice, the "superior" performance of electronic circuits simulators and the complexity of both analog circuits and electronic devices models make such an approach useless. We mention that in some cases, for a given non-electrical system, different equivalent electric circuits may be found; a detailed discussion of modelling non-electrical systems with equivalent electrical systems may be found in [3,49].

Finally, in many practical cases, ideal "analog behavioural models" may be useful for building SPICE models of non-electrical systems (see later).

5.1. Equivalent electric circuits for thermal systems

A given thermal system may be translated into an equivalent electric circuit by using the following equivalence table

$$P \leftrightarrow I, \qquad \Delta T \leftrightarrow \Delta V, \qquad R_{TH} \leftrightarrow R, \qquad C_{TH} \leftrightarrow C \quad (22)$$

where for each signal or component in the thermal domain (left) there is an associated electrical signal or component in the electrical domain (right).

As an example, let us consider an object which is heated by a power P_0; for simplicity we assume that all the volume of the object is at the same temperature. In the thermal domain, the object has its temperature and is separated from the surrounding environment by a thermal resistance; furthermore, it has its thermal capacitance. Assuming that the environment temperature be constant, a simple correspondent equivalent electric circuit may be found by defining a node for each volume with a different temperature and using the equivalence (22), as shown in Fig. 4.

5.2. Equivalent electric circuit for a vibrating capacitor

The Kelvin Probe is a very convenient method for the measurement of the work function of a given material [50–55], as it guarantees surface integrity and can be used for a very wide range of materials, temperatures and pressures [50]. In Kelvin Probe systems, a voltage V_X is applied across a capacitor whose plates are constituted, respectively, by a reference material, A, and by the sample material, B, whose work function is unknown. The charge Q stored in the capacitor is

$$Q = C[V_X - \Delta\Phi_{AB}] \quad (23)$$

where $\Delta\Phi_{AB}$ is the contact potential difference (corresponding to the work function difference $q\Delta\Phi_{AB}$) and C is the capacitance. If the capacitance C is somehow time-dependent and V_X is constant, the current through the capacitor (also called the Kelvin current) is

$$i_C(t) = \frac{dQ(t)}{dt} = \frac{dC(t)}{dt} \times [V_X - \Delta\Phi_{AB}] \quad (24)$$

The voltage V_X may then be changed (slowly, as our derivation assumed a constant V_X) until the Kelvin current is zeroed, which gives $V_X = \Delta\Phi_{AB}$; in this way the contact potential difference may be measured. In practice, a time-dependent capacitance may be obtained in different ways: for a parallel plates capacitor ($C = A\varepsilon/d$) the dielectric time constant, ε, the area of the capacitor, A, or the distance between the two plates, d, may be varied; although all these methods have been explored, the most practical one consists in using a time-dependent distance (vibrating capacitor); as an example, let us consider

$$d(t) = d_0 + d_1 \sin(\omega_0 t) \quad (25)$$

Fig. 5 shows a SPICE model for such a vibrating capacitor [55]. The voltage-controlled voltage source E1 gives, at the output, the difference $(V_X - \Delta\Phi_{AB})$ which is multiplied by $C(t)$; the resulting signal is then derived and fed into the voltage-controlled current source G1 which produces the Kelvin current. Interestingly, this model takes advantage of an ideal "analog behavioural model" (which performs the operation "1/x"). The accuracy of this simple model has been experimentally verified, as shown in Fig. 6a and b [55].

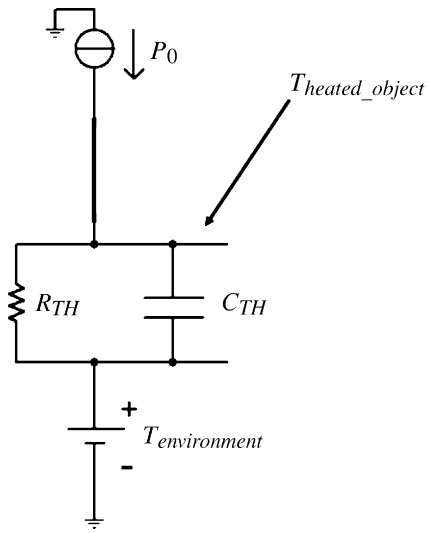

Fig. 4. Equivalent electric circuit of a simple thermal system.

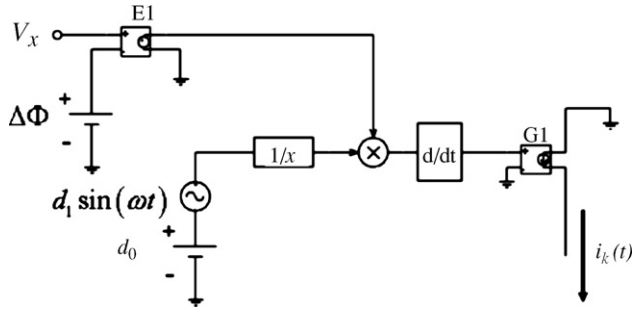

Fig. 5. SPICE model of a vibrating capacitor.

6. Technological issues

Electronic interfaces may employ integrated circuits (IC) and/or discrete components; discrete components may be preferable for fast prototyping and for small volumes production, while integrated circuits may allow higher performance (speed, low power, interferences rejection, etc.) and much lower costs for large volumes. In some applications, even if the interface must be integrated, a few auxiliary discrete components may be required for achieving the desired level of accuracy. In practice, there are many technological options for fabricating integrated electronic interfaces.

Sensors realized with silicon based technologies can detect various physical and chemical quantities with acceptable sensitivity. Since these technologies exploit the same materials (silicon, polysilicon, metal and dielectrics) and processing steps as standard integrated circuits, the evolution toward microsystems or assembled micromodules, including sensing devices and

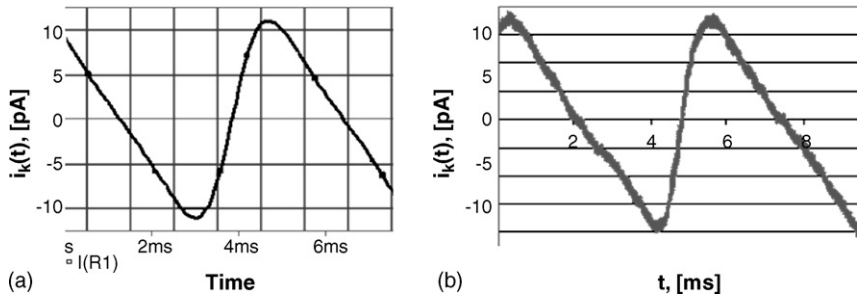

Fig. 6. (a) Current generated by the SPICE model of a vibrating capacitor. (b) Measured current generated by a vibrating capacitor.

interface circuits on a single chip or in a single package, is straightforward [1,56–60]. The advantages of this approach are numerous: the cost of the sensing system is greatly reduced due to batch fabrication, its size and interconnections are minimized and its reliability is improved.

However, the choice of materials compatible with silicon technologies is limited and, therefore, integrated sensors are often less performant than discrete devices, because of weak signals, offset and non linearity and, hence, introduce increasing demands on the electronic interface circuits [61], requiring an intensive use of the circuit techniques described in the next section.

Depending on the specific application, the design of integrated sensors systems may be extremely challenging for different reasons: technological constraints, the low level of the sensor signals, the aggressive environment, the required signal processing functions, low power consumption for extended autonomy, etc. In any case, it is usually important that the microsensor, the interface circuit and, often, the package be designed together. Indeed, the optimum microsystem or micromodule is not necessarily obtained by interconnecting separately optimized sensors and interface circuits. Microsensor interface circuit design, therefore, requires specific and interdisciplinary knowledge as well as special techniques in order to achieve the reliability and the performance demanded by the user.

As mentioned above, there are two possible solutions for implementing smart sensor systems: the "microsystem" approach and the "micromodule" approach.

In the microsystem approach, the sensor and the electronic interface circuitry are integrated on the same chip, as shown in Fig. 7. In this case the complete system is obtained using a standard IC (integrated circuits) process with, eventually, a few compatible post-processing steps (typically etching or deposition of materials). Therefore, the microsensor has to be designed taking into account the material features (layer thickness, doping concentrations and design rules) imposed by the standard IC process used (CMOS, bipolar or BiCMOS); any additional processing step required for implementing the sensing devices has to be performed after the completion of the standard IC fabrication flow. Obviously, this situation reduces the degrees of freedom available for sensor design, thus introducing additional challenges. Moreover, especially when using scaled-down (submicron) technologies, this approach can introduce cost and yield problems. Indeed, the silicon area occupied by the electronic interface circuit typically shrinks with the feature size of the technology, while the sensor area in most cases remains constant, since it is determined by "physical" considerations, such as the mass of the structures or the angle of etched cavities, which are not changed by improvements in the technology. Therefore, while for integrated circuits the increasing cost per unit area is abundantly compensated by the reduction in the area, leading to an overall reduction of chip cost with the technology feature size, this might not be true for integrated microsystems. Moreover, a defect in the sensors may result in the failure of the complete microsystem even if the circuitry is working properly, hence lowering the yield and again increasing the cost (the yield for sensors is typically lower than for circuits).

The microsystem approach, however, also has considerable advantages. First of all, the parasitics due to the interconnections

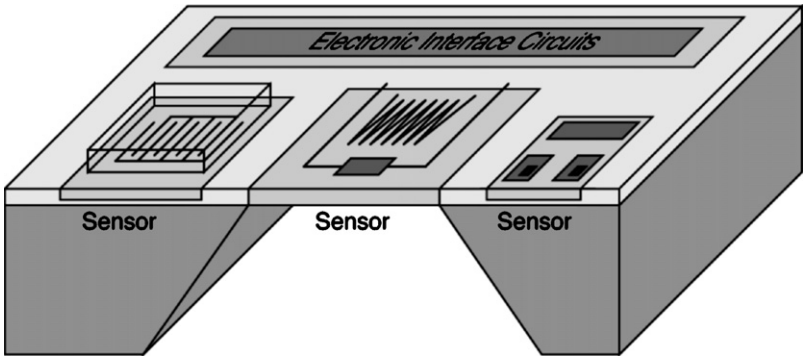

Fig. 7. Smart sensor system (microsystem approach).

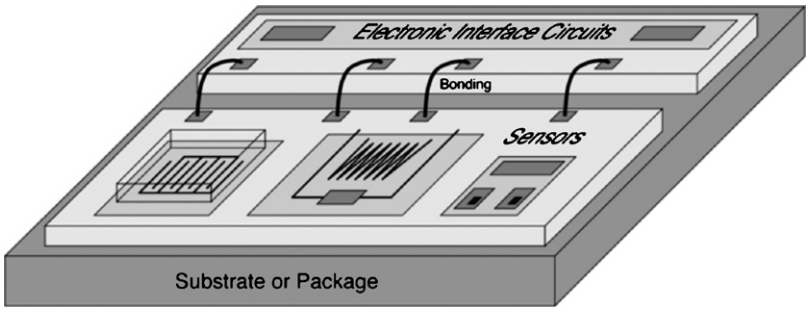

Fig. 8. Smart sensor system (micromodule approach).

between sensors and electronic interface circuits are minimized and, more important, well defined and reproducible, which is very beneficial for the system performance. Moreover, the system assembly is simple, inexpensive and independent of the number of connections needed because all the interconnections are implemented during the IC fabrication process. Finally, when required, the use of the same technology allows us to achieve good matching between elements of the sensor and those of the interface circuitry, thus allowing an accurate compensation of many parasitic effects.

In the micromodule approach the sensors and the electronic interface circuits are realized on different chips. They are included in the same package or mounted on the same substrate, as shown in Fig. 8. The interconnections between the sensor chip and the electronic interface circuit chip can be realized with bonding wires or with other techniques, such as flip-chip or wafer bonding. With this approach the two chips can be implemented with different technologies, optimized for the sensors and the circuitry, respectively. Typically, expensive submicron technologies are used to realize the electronic interface circuits, while low cost technologies with large feature size and few masks are used for implementing the sensors. In this case, the material properties of the technology can be adjusted to optimize the performance of the devices. The cost and yield issues mentioned for the microsystem approach are not any longer important.

However, the micromodule approach has also drawbacks. First of all, the assembling of the system can be quite expensive and unreliable, allowing only a limited number of interconnections between the sensor and the electronic interface circuits. Moreover, the parasitics due to the interconnections are orders of magnitude larger, more unpredictable and less repeatable than in the microsystem approach, thus eventually neutralizing the sensor performance improvements obtained with technology optimization. Finally, no matching between elements of the sensor and elements of the electronic interface circuitry can be guaranteed.

From the above considerations it is evident that both approaches have merits and drawbacks. The choice of the approach substantially depends on the application, the quantity to be measured, the kind of sensors, the specifications of the electronic interface circuits and the available fabrication technologies, thus producing a number of trade-offs, which have to be analyzed before taking a decision.

7. Techniques for high accuracy and high precision electronic interfaces

7.1. Feedback

High accuracy electronic interfaces almost invariably take advantage of feedback. In fact, electronic interface contain active devices, whose parameters are generally inaccurate, due to the unavoidable spread of process parameters and to drift (aging and variations of the operative conditions such as temperature, supply voltages, etc.); in fact though each parameter (e.g. the current gain of a bipolar transistor) has its average value, in practice, we are interested in the accuracy of a *single* interface, and, therefore, in the accuracy of *single* devices (and we do not care about hypothetical "average" electronic interfaces and "average" devices).

The solution to this issue is a proper use of feedback; the basic (single input single output) linear feedback system is represented in Fig. 9; each block has its own transfer function which, in general, depends on the frequency; the linearity hypothesis is implicit as transfer functions may only be defined for linear, time invariant systems.

In the case of electronic circuits the input signal, x_{in}, the feedback signal, x_f, and the error signal, x_e, may be either voltages either currents (however they must be homogeneous so that $x_e = x_{in} - x_f$); in the same way, the output signal, y_{out}, may be either a voltage either a current.

In general, the block A comprises a number of active devices, and therefore its transfer function is not very accurate; on the contrary the block β is generally made of passive devices and its transfer function may be rather accurate. It may be easily found that the closed loop transfer function of the feedback system in Fig. 9 is given by

$$A_{CL} = \frac{y_{out}}{x_{in}} = \frac{A}{1 + A\beta} \tag{26}$$

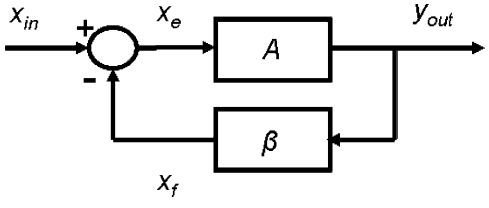

Fig. 9. Block scheme for a feedback system.

so that, at frequencies where the magnitude of the *loop gain* $|A\beta|$ is much larger than 1, the closed loop transfer function may be well approximated as follows

$$[|A\beta| \gg 1] \Rightarrow \left[A_{CL} = \frac{y_{out}}{x_{in}} = \frac{A}{1+A\beta} \simeq \frac{1}{\beta}\right] \tag{27}$$

The last expression clearly illustrates the great advantages of feedback systems from the point of view of accuracy: provided that the magnitude of the loop gain is enough high, the accuracy of the feedback system (i.e. the accuracy of the closed loop transfer function) is mainly related to the accuracy of the feedback network (made of passive devices, whose parameters are generally much more accurate than parameters of active devices). As a simple example, let us consider the voltage–voltage feedback system shown in Fig. 10 (which is obtained from the general system in Fig. 9, when x_{in}, x_f, x_e, and y_{out} are voltage signals). Here, let us assume that, in a certain bandwidth B,

$$10^4 \leq A \leq 10^6, \qquad \beta = \frac{1}{10} \tag{28}$$

Clearly, in the bandwidth B the magnitude of the *loop gain* $|A\beta|$ is much larger than 1, so that the approximate relation (27) is rather accurate and, therefore, despite the large variations of A, for all frequencies in the bandwidth B

$$A_{CL} = \frac{v_{out}}{v_{in}} = \frac{A}{1+A\beta} \simeq \frac{1}{\beta} = 10 \tag{29}$$

Since this analysis is general, feedback helps to counteract the variations of A independently on the causes of those variations (temperature, spread of parameters, supply voltage, input common mode range voltages, frequencies, etc.).

Let us now derive a simple circuit implementation of the voltage–voltage feedback system shown in Fig. 10; for simplicity we assume that an ideal differential amplifier, with voltage gain A, is available (since the differential amplifier is ideal, it has zero input currents, zero output impedance, infinite common mode and power supply rejection ratios, etc.). The differential amplifier may replace both the block A and the adder of the block scheme in Fig. 10 (in fact, it computes the difference between two voltage signals and then amplifies it by A); as to the block β, it is a voltage attenuator (in our example $\beta = 1/10$) whose input is the output voltage of the feedback system and whose output is the feedback voltage signal; the voltage attenuator β may then be replaced by a voltage resistive divider as shown in Fig. 11.

Although feedback is a powerful tool for the design of high accuracy analog circuits and electronic interfaces, it also has

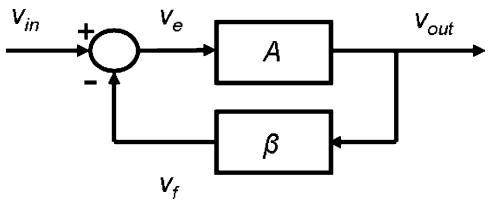

Fig. 10. Block scheme for a voltage input–voltage output feedback system.

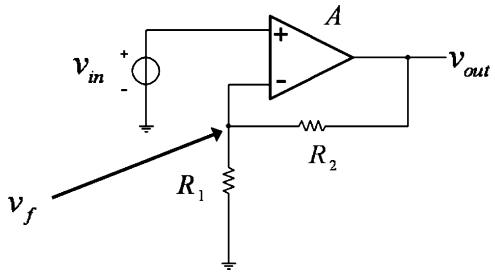

Fig. 11. A circuit using voltage input–voltage output feedback.

its limits. First, the presence of feedback paths introduces the risk of auto-oscillation which, in the case of an amplifier, is unacceptable; here we only mention that the higher the number of gain stages, the more problematic this inconvenient [62–72]. Second, the accuracy of a feedback system is still limited because of the limited loop gain. In particular, if we consider the output and the ideal output signal of the feedback system,

$$y_{out} = \frac{A}{1+A\beta}x_{in}, \qquad y_{out,ideal} = \frac{1}{\beta}x_{in} \tag{30}$$

we may find the ideal and real sensitivities, the sensitivity error S.E., and the relative sensitivity error R.S.E. (if the input and the output signals are homogeneous, the sensitivity is a gain)

$$S_{ideal} = \frac{1}{\beta}, \qquad S = \frac{A}{1+A\beta},$$
$$\text{S.E.} = S - S_{ideal} = \frac{-1}{(1+A\beta)\beta},$$
$$\text{R.S.E.} = \frac{S - S_{ideal}}{S_{ideal}} = \frac{-1}{(1+A\beta)} \tag{31}$$

If the magnitude of the loop gain is much larger than 1, the relative sensitivity error may be approximated as

$$\text{R.S.E.} = \frac{S - S_{ideal}}{S_{ideal}} = \frac{-1}{1+A\beta} \simeq \frac{-1}{A\beta} \tag{32}$$

which is an important relation. For instance, with reference to the circuit shown in Fig. 11, if we consider the two systems

$$A_1 = 10^6, \qquad \beta_1 = \frac{1}{10}, \qquad A_2 = 10^4, \qquad \beta_2 = \frac{1}{10} \tag{33}$$

we immediately find (in this case the sensitivity is a gain)

$$|\text{R.G.E.}_1| \simeq 10^{-5}, \qquad |\text{R.G.E.}_2| \simeq 10^{-3} \tag{34}$$

Finally, we mention that a proper application of feedback also helps to modify the impedance level; this observation may be extremely useful in the design of electronic interfaces (for instance, see later how feedback helps to measure high impedances in the next section).

7.2. Compensation of amplifiers non idealities

Real amplifiers, even when feedback is properly applied, still introduce errors which may dominate the error of the complete measurement systems. In principle, it is possible to reduce this

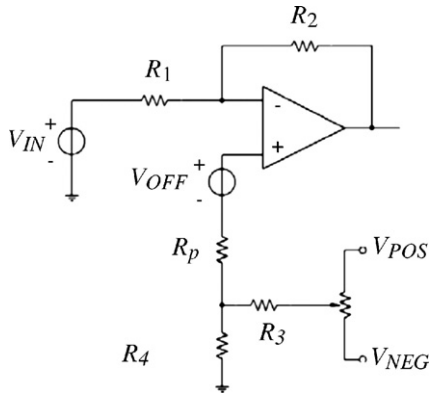

Fig. 12. A circuit for the compensation of both the input offset voltage and the input currents of the op amp.

type of errors by tuning some component values; as an example, Fig. 12 shows a classic solution for compensating both the input offset voltage and the input currents of the op amp by means of a potentiometer. There are two reasons which severely limit the applicability of these static techniques in electronic interfaces. First, tuning increases the costs; in integrated circuits produced in large volumes, the cost of an eventual tuning procedure may be comparable with the cost of chip fabrication. Second, tuning is a "static" technique, and, hence, may not compensate errors which evolve with time, such as noise, thermal drift, aging, etc. Nevertheless, static techniques may still be convenient in some cases (e.g. fast prototyping, small volumes products, etc.).

In general, it is possible to compensate the amplifiers non idealities by means of dynamic (or automatic) compensation techniques. These dynamic compensation techniques are especially important for CMOS interfaces; in fact, in many practical cases, low cost and compatibility with digital systems make it very convenient to integrate electronic interfaces in standard CMOS processes; however, due to the relatively poor quality of CMOS transistors it is generally required to somehow compensate the non idealities of CMOS amplifiers. Static techniques would be too expensive and useless, as they might not reduce time-varying errors such as the low frequency noise and drift, which in CMOS systems are relevant. These reasons and the availability in CMOS processes of low cost high performance switches have made automatic (or dynamic) techniques for compensating non idealities of amplifiers almost ubiquitous in CMOS systems. Although some attempts have been made to classify these techniques [73–76], these classifications are not completely correct, resulting in some confusion and, eventually, in sub-optimal designs; here we shortly discuss a more correct classification [77–80].

Autozero circuits (AZCs) require sampling (compensation phases) and, afterwards, accurate signal processing (the auxiliary signals sampled in the compensation phases compensate the errors in the signal processing phases) [73,74]. Fig. 13 shows a simple amplifier which implements the autozero principle; in fact, assuming that the low frequency input noise voltage does

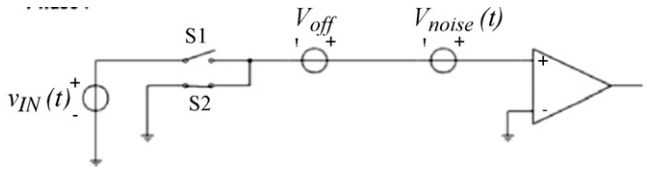

Fig. 13. Autozero amplifier (basic circuit).

not significantly change during one "autozero period", we find

$$V_{\text{out,I}} = A[v_{\text{IN}}(t_x) + V_{\text{off}} + V_{\text{noise}}(t_x)],$$
$$V_{\text{out,II}} = A[V_{\text{off}} + V_{\text{noise}}(t_x + \Delta t)],$$
$$V_{\text{noise}}(t_x + \Delta t) \cong V_{\text{noise}}(t_x) \Rightarrow V_{\text{out,I}} - V_{\text{out,II}} \cong A v_{\text{IN}}(t_x) \tag{35}$$

Autozeroing may reduce the effects of the input offset and $1/f$ noise voltages and of the finite gain of amplifiers; in principle, autozeroing might also reduce any other non ideality which does not significantly change during one "autozero period"; for instance, dynamic current mirrors and instrumentation amplifiers (IA) employing the "flying capacitor" (for improving the CMRR) may also be regarded as autozero circuits. Another powerful application of the autozero technique is the three signals approach, which is graphically described in Fig. 14; in this circuit we find

$$V_{\text{out,I}} = A[v_{\text{IN}}(t_x) + V_{\text{off}} + V_{\text{noise}}(t_x)],$$
$$V_{\text{out,II}} = A[V_{\text{off}} + V_{\text{noise}}(t_x + \Delta t)],$$
$$V_{\text{out,III}} = A[V_{\text{REF}} + V_{\text{off}} + V_{\text{noise}}(t_x + 2\Delta t)],$$
$$V_{\text{noise}}(t_x + 2\Delta t) \cong V_{\text{noise}}(t_x + \Delta t) \cong V_{\text{noise}}(t_x)$$
$$\Rightarrow v_{\text{IN}}(t_x) \cong \left(\frac{V_{\text{out,I}} - V_{\text{out,II}}}{V_{\text{out,II}} - V_{\text{out,III}}}\right) V_{\text{REF}} \tag{36}$$

The last expression in (36) clearly shows how the input signal may be deduced independently on the input offset voltage, on the low frequency noise, and on the amplifier gain; as it is clear from (36), the three signals approach requires a system which may accurately compute the ratio between two signals (e.g. a microprocessor).

Although autozeroing allows, in principle, to compensate any kind of error which is (almost) constant during the autozero period, it also results in larger residual noise, because the input equivalent thermal (i.e. wideband) noise is under-sampled [73,81].

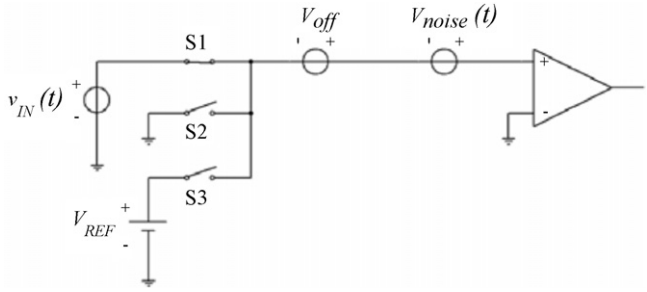

Fig. 14. Three signals approach.

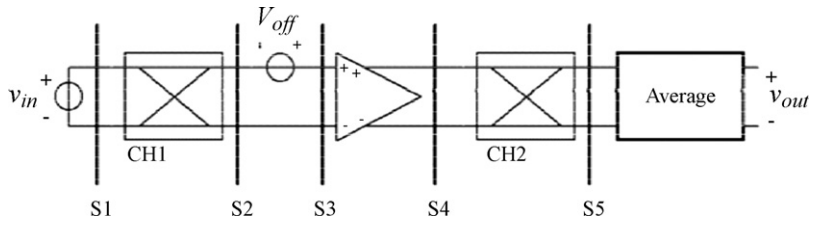

Fig. 15. CMOS chopper amplifier.

Chopper circuits (CHCs) reduce the effects of the input offset and low frequency noise of amplifiers by means of chopper switches which enable a modulation–demodulation technique, as shown in Fig. 15 (the "choppers" CH1 and CH2 enable the straight connections during one phase and the crosswise connection during the other phase). In practice, the chopper switches modulate the input signal, amplify the modulated signal, and demodulate the (modulated and amplified) signal. As a result the signal is modulated, amplified and then demodulated back to the base band; on the contrary, the input offset and 1/*f* noise voltages of the amplifier are only amplified and modulated and, therefore, may be removed by low pass filtering. Although different (e.g. sinusoidal) modulation–demodulation strategies would allow the compensation of the input offset and low frequency noise of amplifiers, chopper circuits are very convenient in CMOS systems as high performance switches are easy to be implemented. Since no sampling occurs, chopper circuits are continuous time systems and there is no under-sampling of the thermal wideband noise.

Although the absence of sampling results in a lower residual noise, in comparison with AZCs, CHCs may not compensate the finite open loop gain, the output resistance, etc. Interestingly, for very low frequency electronic interfaces, the nested chopper technique [74,75,82] allows a further reduction of the residual amplifier offset down to 100 nV; the application of such a technique is, however, limited to those applications where one can make sure that other sources of errors, such as spurious thermocouple effects, do not dominate the residual offset [74].

Circuits which use dynamic element matching (*DEMCs*) take advantage of the following principle: if the error is mainly due to the mismatch between some devices, it is possible to reduce the error by dynamically matching [83] those devices (that is dynamically interchanging the "mismatched"devices and taking the average). Dynamic element matching of active devices may be combined with dynamic matching of feedback elements [84,85], thus rejecting errors due to resistance (or capacitance) ratios errors (especially important for high temperature applications [84]).

Within these definitions, in contrast with traditional classifications [73–76], chopper and dynamic element matching are different techniques. As an example, in a folded cascode op amp many transistor pairs contribute to the input offset voltage; it is then better, in order to reduce the offset, to dynamically interchange all those transistors pairs (and not only the input transistors); the resulting circuit is DEMC but not CHC. However, the amplifier shown in Fig. 16 may be regarded both as a CHC (the chopper switches act as the modulators) or as a DEMC (the input transistors are interchanged during the two phases). Fig. 17 shows the generally accepted classification and the more correct classification [77–80] for automatic techniques: although some overlap exists between CHCs and DEMCs, these are different classes. We mention that, although our discussion embraces the most common dynamic techniques, other techniques have also been proposed (e.g. switched biasing [86]).

The differences between the classifications shown in Fig. 17 are not just a matter of nomenclature; for instance, dynamic element matching also allows the compensation of the finite op amp gain without autozeroing (which has been believed not possible [73]); this is an interesting opportunity for those applications where the op amp gain may not be too high, which is often the case in deep sub-micrometer CMOS microsystems. As an example, assuming that one has two identical op amps, it is possible to design a circuit where errors (including finite gain errors) generated by one op amp effectively compensate the errors generated

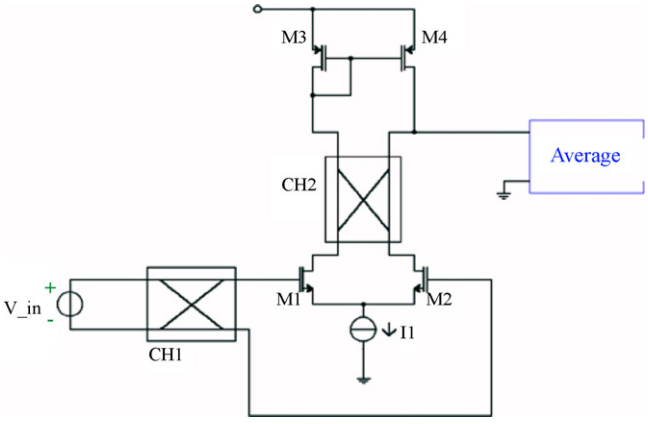

Fig. 16. A simple CMOS chopper differential amplifier.

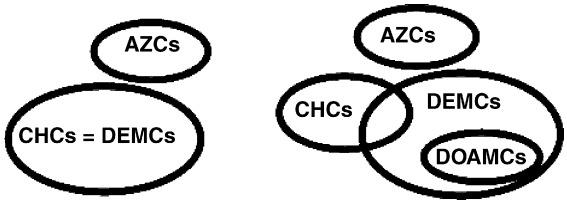

Fig. 17. Classifications of automatic compensation techniques for CMOS amplifiers.

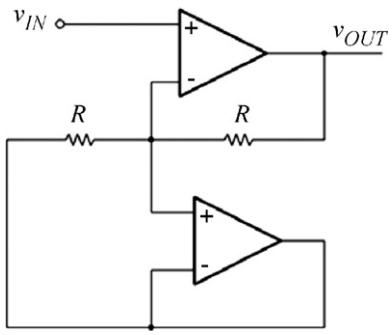

Fig. 18. Dual op amp buffer.

by the second op amp; for instance, Figs. 18 and 19 show two circuits which implement this idea for, respectively, a voltage buffer [77,78,87,88] and a differential amplifier [89]; these circuits would allow, in case of ideal op amp matching, a strong reduction of the finite op amp gain; however, since practical op amps show mismatch, dynamic element matching must be applied to the entire op amps (dynamic op amp matching); if these circuits are properly designed, the input offset and noise voltages and also the finite open loop gain of op amps are compensated without autozeroing, resulting in a lower residual noise. Nevertheless, the presence of two op amps results in an equivalent input root mean square (rms) noise voltage which is $\sqrt{2}$ times larger than the correspondent voltage of an equivalent chopper circuit. Dynamic op amp matching should be avoided if the op amp gain is enough large (in these cases chopper or traditional dynamic element matching circuits would give a lower residual noise). In comparison with other techniques, dynamic op amp matching circuits contain multiple feedback loops; however proper circuit transformations make their frequency compensation straightforward (even if their "equivalent" open loop gain is very large). It should be noted that, though a static technique such as the so called op amp tuning [90] may also reduce the mismatch between op amps, it would not compensate the 1/*f* noise which, in CMOS interfaces, is often a main issue.

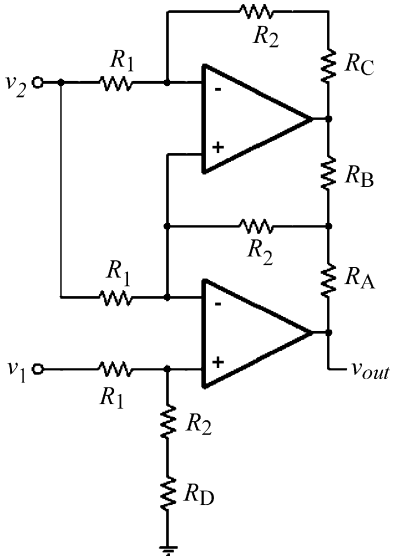

Fig. 19. Dual op amp differential amplifier.

Finally, we mention that the application of the dynamic element matching to a second generation current conveyor (CC-II) [91] is another approach which does not require autozeroing and, in principle, might allows to integrate accurate and precise interfaces based on low gain CMOS amplifiers; in these circuits dynamic element matching must also be applied for compensating the mismatch and 1/f noise of the transistors which are outside the loop; with reference to Fig. 17, these circuits also belong to the class of DEMCs, but not CHCs.

7.3. Signal to noise ratio (SNR) enhancement

In some cases the signal levels to be measured are extremely small; it is even possible that the power of the superimposed noise and interferences is larger than the power of the signal of interest. In such circumstances special techniques for enhancing the signal to noise ratio should be considered, such as:

(1) lock-in amplifiers (analog or digital)
  (1.a) with only one reference frequency
  (1.b) eterodine lock-in with two or more reference frequencies
  (1.c) high frequency lock-in
(2) waveform averagers
  (2.a) signal averagers
  (2.b) box car integrators
  (2.c) waveform eductors
(3) auto-correlators and cross-correlators

All these solutions somehow reduce the noise bandwidth. Here we only consider the lock-in amplifier operating with a single reference frequency because it is widely used in electronic interfaces, and also because its integration by silicon technologies has already been proven.

Lock-in amplifiers are AC voltmeters which measure the amplitude of an AC signal at a reference frequency, f_0, even when the power of this AC signal is extremely small and, eventually, smaller than the power of environmental interferences. The lock-in amplifier needs a reference signal which provides the reference frequency, f_0; ideally, the output of the lock-in is a DC signal proportional to the component of the input signal which has the same frequency as the reference signal.

Let us consider a signal of interest

$$v_s = V_{s0}\sin(2\pi f_0 t + \varphi_0) \tag{37}$$

Due to various interferences and noise processes, the signal of interest may be contaminated by a "wideband" additive disturb, v_D; since the spectrum of the signal of interest is zero for all frequencies but f_0, a proper bandpass filter (center frequency equal to f_0) might greatly increase the signal to noise ratio; for instance, an hypothetical filter which blocks all the frequencies

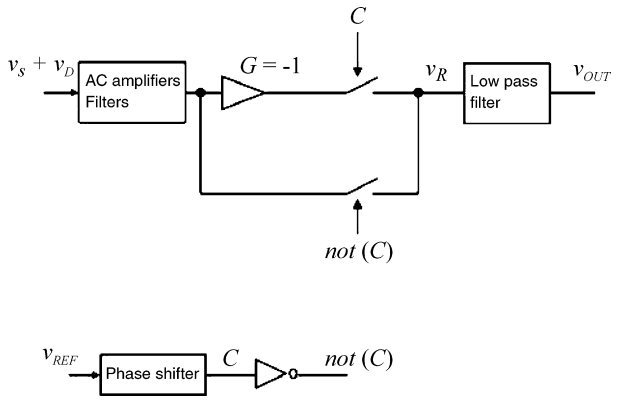

Fig. 20. A simple implementation of the lock-in amplifier.

but f_0 would completely remove the disturb (assuming that the disturb has a negligible component at the frequency f_0). However, for a significant enhancement of the signal to noise ratio, the Q of the bandpass filter should be very large; even assuming that one may implement a very high Q filter (which is not easy), it would then be extremely difficult to tune the center frequency of the filter (this would be critical because a very small difference between this frequency and f_0 would result in large errors). These difficulties may be overcome by means of the so called lock-in amplifiers, which take advantage of a reference signal v_{REF}, at the same frequency as the signal of interest, for implementing a synchronous demodulation of the input signal; although a signal with the same frequency as the signal of interest is generally available, a phase shifter must be used in order to zero the phase difference between the reference signal and the signal of interest.

A simple implementation of the lock-in technique is shown in Fig. 20. Here, the phase shifter may change the phase difference between the reference signal and the signal of interest; the output of the phase shifter, C, is passed through an inverter so that these two anti-phase control signals may drive the correspondent switches. As evident from Fig. 21, if the phase difference between the reference signal and the signal of interest is 0 or 180°, the signal v_R has a non-zero DC component which is proportional to V_{s0}; the DC component of v_R may easily be extracted by means of a suitable low pass filter.

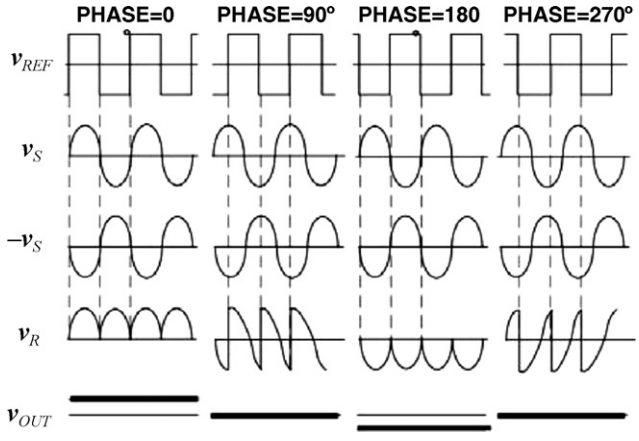

Fig. 21. Signals in the lock-in amplifier shown in Fig. 20 for various phase differences between the signal of interest and the reference signal.

Interestingly, lock-in amplifiers can be seen as very narrow filters with a central frequency f_0 and a quality factor Q which can be expressed as $Q = (f_0/\Delta f)$ where Δf is the bandwidth of the low pass filter. Obviously, the smaller the bandwidth of the low pass filter, the higher both the Q and the rejection of the disturbances; on the other hand, the complete system may not be faster than the low pass filter itself, so that a trade-off exists between the Q (which is related to the disturbance rejection) and the speed of the lock-in amplifier (in other words, an accurate measurement requires a long measurement time).

The SNR improvement achieved through the use of the lock-in amplifier is the ratio between the SNR at the output and the SNR at the input. This improvement can also be expressed as the square root of the signal source bandwidth divided by the equivalent noise bandwidth of the lock-in amplifier. The SNR at the output of the lock-in amplifier is given by the SNR at the input multiplied by the square root of the ratio between the noise bandwidth and the bandwidth of the low pass filter; as an example if the noise bandwidth is 10^4 Hz and the bandwidth of the low pass filter is 10^{-2} Hz, the S/N improvement is 10^3.

Finally, we mention that it is possible to conveniently integrate several basic lock-in functions into a single chip [92,93].

7.4. Measurement of low and high impedances

Here we describe two general techniques which are useful when the sensor impedances are very small (so that series parasitic resistances may not be neglected) or very high (so that shunt parasitic impedances may not be neglected). Although in the next section we shall discuss interfaces for resistive sensors in more detail, for simplicity, it is better to consider the simple interface shown in Fig. 22; in this interface the current I_0 is injected into the sensor resistance R_X, thus producing a voltage

$$v_{IN,AMP} = R_X I_0 \tag{38}$$

at the input of the voltage amplifier. In practice, if the sensor resistance is very small (and/or the sensor resistance is far from the interface), the series parasitic resistances may not be neglected (see Fig. 23) and the input voltage of the amplifier becomes

$$v_{IN,AMP} = (R_{P1} + R_X) I_0 \tag{39}$$

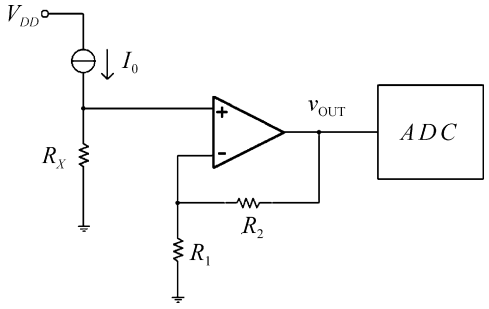

Fig. 22. A simple interface for a resistive sensor.

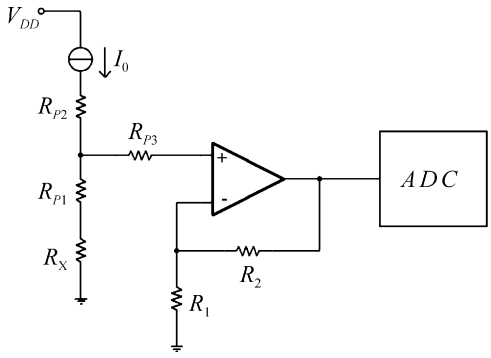

Fig. 23. Effect of parasitic series resistances.

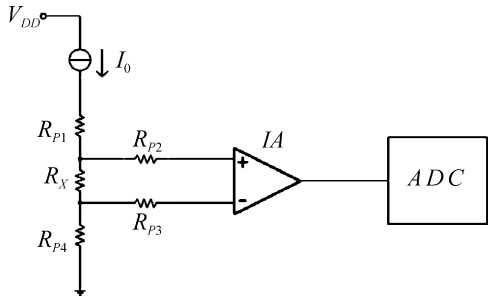

Fig. 24. Four-wires measurement of a resistance.

It must be observed that the parasitic resistances R_{P2} and R_{P3} do not introduce any error; more accurately, this is, strictly, true if the op amp has zero input currents and the current source has infinite output impedance (it is generally possible to make sure that both these hypotheses are good approximations). It must also be noted that, even if, in principle one could "calibrate" the error due to R_{P1}, the variations of R_{P1} (with temperature, humidity, ...) may still degrade the accuracy of the measurement.

A simple solution is the four-wires approach (also called Kelvin method) shown in Fig. 24. Here, due to the negligible input currents of the instrumentation amplifier *IA* (which generally contains two or three op amps), the input voltage of the amplifier is exactly

$$v_{IN,AMP} = R_X I_0 \tag{40}$$

The complementary problem is found when measuring very high impedances, as shown in Fig. 25; here a part of the current I_0 flows across the parasitic resistance R_P, so that the input voltage

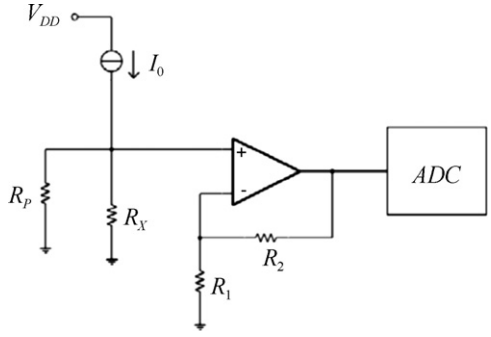

Fig. 25. Effect of parasitic shunt resistances.

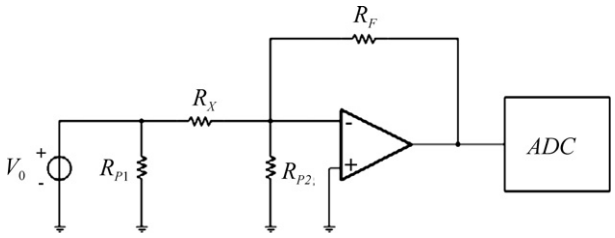

Fig. 26. A circuit which is insensitive to parasitic shunt resistances.

of the amplifier is

$$v_{IN,AMP} = (R_X // R_P) I_0 \tag{41}$$

A convenient solution to this problem takes advantage of feedback and is shown in Fig. 26; here, both the shunt parasitic resistances must be considered because neither terminal of the sensor resistance is connected to ground; however, if, for simplicity, we consider an ideal op amp, the voltage at the negative input terminal of the op amp, v_-, is zero, so that the current through the sensor resistance is

$$i_{RX} = \frac{V_0}{R_X} \tag{42}$$

Since there may be no current through R_{P2} (because v_- is zero), the current i_{RX} entirely flows through R_F and the output voltage of the op amp is

$$v_{OUT} = \frac{-V_0 R_F}{R_X} \tag{43}$$

which does not depend on the parasitic resistances.

8. Case studies

8.1. Resistive sensor interfaces

Interfaces for resistive sensors generally use either a resistance to voltage conversion if the resistance variations are relatively small, or a resistance-to-period (or, equivalently, resistance-to-frequency) conversion if the resistance variations are very large (e.g. more than about 3 decades). As an example, platinum resistive temperature sensors typically exhibit rather low relative resistance variations. On the contrary, metal oxide resistive gas sensors may change their resistance by orders of magnitude as a consequence of physisorption, chemisorption and catalytic reactions (e.g. the interaction with oxidizing gases, such as NO_2 and O_3, increase the resistance of *n-type* metal oxides like SnO_2 and WO_3 [94], and decrease the resistance of *p-type* metal oxides like NiO and CoO [95,96]).

The Wheatstone bridge (Fig. 27) is a very simple circuit for converting resistance variations into a differential voltage signal; this method was proposed by S.H. Christie in 1833 and subsequently reported by Sir C. Wheatstone to the Royal Society (London) in 1858. In general, one or more resistors of the Wheatstone bridge may be sensitive to the measurand; in most practical cases there is only one sensor. The sensor resistance is generally placed in one of the four branches of the bridge; if, for a given value of the measurand, the bridge is balanced (i.e.

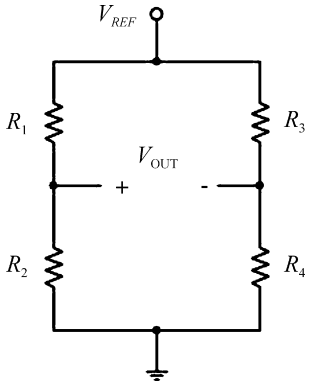

Fig. 27. Wheatstone bridge.

$(R_1/R_3) = (R_2/R_4)$, so that the differential voltage V_{out} is zero), a variation of the measurand will unbalance the bridge. As a practical example, let us consider the Wheatstone bridge shown in Fig. 28; here there is only one sensor which has a resistance

$$R_0(1 + x) = R_0 + xR_0 \tag{44}$$

where R_0 is the base-line resistance, x the relative resistance variation, and xR_0 is the resistance variation. The differential output voltage of the bridge is

$$V_{\mathrm{OUT}} = V_{\mathrm{REF}} \frac{x}{4 + 2x} \tag{45}$$

If the relative variation of the sensor resistance, x, is low, there is an almost linear relation between the differential output voltage and the relative variation of the sensor resistance, as

$$V_{\mathrm{OUT}} = V_{\mathrm{REF}} \frac{x}{4 + 2x} \simeq V_{\mathrm{REF}} \frac{x}{4} \tag{46}$$

It must be stressed that, depending on the definition, different expressions (and dimensional units) may be appropriate for the sensitivity of the same interface. As an example, the Wheatstone bridge shown in Fig. 28 may be regarded as a converter from resistance variation, xR_0, to differential voltage, with sensitivity given by

$$\frac{\partial V_{\mathrm{OUT}}}{\partial [xR_0]} \simeq \frac{V_{\mathrm{REF}}}{4R_0} \left[\frac{\mathrm{V}}{\Omega}\right] \tag{47}$$

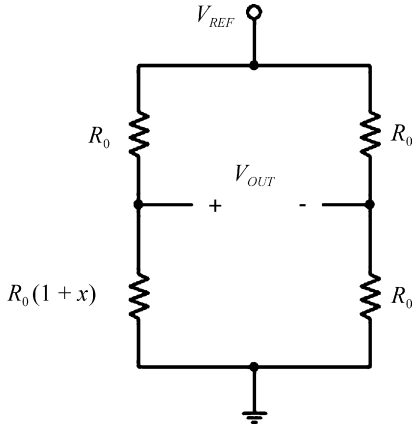

Fig. 28. A Wheatstone bridge with only one sensor.

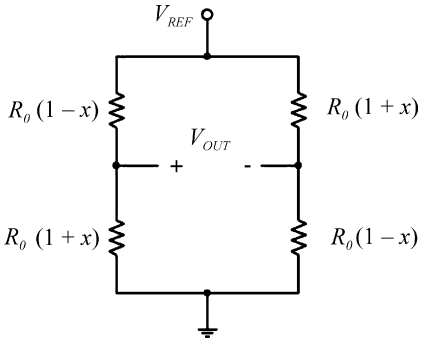

Fig. 29. A Wheatstone bridge with four sensors.

However, the same Wheatstone bridge may be regarded as a converter from relative resistance variation, x, to differential voltage, with sensitivity

$$\frac{\partial V_{\mathrm{OUT}}}{\partial x} = \frac{V_{\mathrm{REF}}}{4}\,[\mathrm{V}] \tag{48}$$

The use of more sensors in the Wheatstone bridge can increase the sensitivity and, eventually, improve the linearity; for instance, Fig. 29 shows a bridge with four sensors, which produces the differential output voltage

$$V_{\mathrm{OUT}} = xV_{\mathrm{REF}} \tag{49}$$

which is perfectly linear with the relative resistance variations of the sensors, x (even for large resistance variations). In this case the sensitivities are, respectively,

$$\frac{\partial V_{\mathrm{OUT}}}{\partial [xR_0]} = \frac{V_{\mathrm{REF}}}{R_0} \left[\frac{\mathrm{V}}{\Omega}\right], \qquad \frac{\partial V_{\mathrm{OUT}}}{\partial x} = V_{\mathrm{REF}}\,[\mathrm{V}] \tag{50}$$

In comparison with the simpler bridge shown in Fig. 28, the Wheatstone bridge using four sensors (Fig. 29) improves the sensitivity (by 4 times) and the linearity; however, in most applications it is difficult, or impossible, to find well matched sensor resistances which show an exactly opposite relative sensor resistance variations in response to the same measurand variation.

If necessary, a differential amplifier may be used for the differential-to-single-ended conversion and for increasing the sensitivity of Wheatstone bridges; clearly, the input currents of the differential amplifier introduce an error; for this reason an instrumentation amplifier is often considered. Fig. 30 shows a very simple circuit which, assuming an ideal op amp, performs

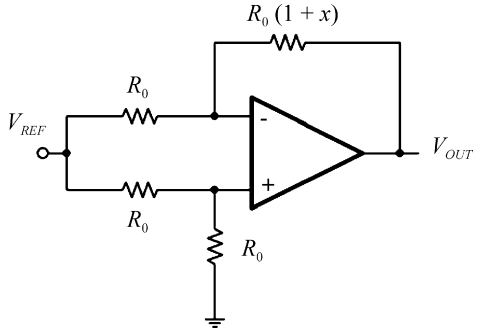

Fig. 30. Interface for a resistive sensor bridge.

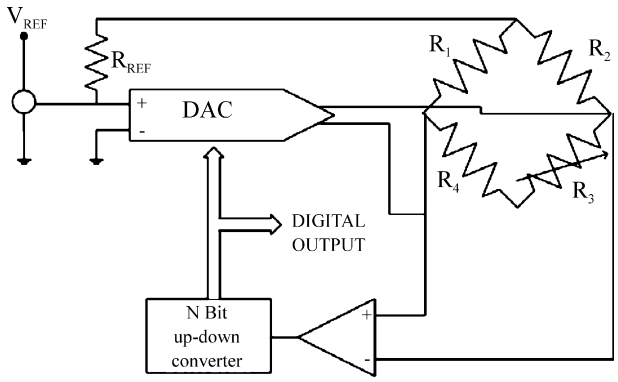

Fig. 31. Wheatstone bridge using a comparison method with automatic balance through DAC.

the differential-to-single-ended conversion and produces an output voltage

$$V_{\mathrm{OUT}} = \frac{-V_{\mathrm{REF}}}{2}x \tag{51}$$

which is exactly linear with the relative resistance variation. A detailed discussion of other interface circuits for resistive sensor bridges may be found in [4].

A Wheatstone bridge may also be interfaced by means of a charge-balancing A/D converter [97,98], thus saving chip area. Fig. 31 shows an alternative approach based on a digital to analog converter (DAC) that produces two complementary current sources: a current corresponding to the digital output and another one corresponding to the complementary digital input. Any imbalance of the bridge output exceeding the comparator threshold modifies the converter outputs through the up-down counter, so that the loop equates the input voltages of the comparator. The system output is the digital word present at the input of the DAC which keeps the bridge balanced [99].

It is also possible to convert the resistive variation into a period (or frequency) [100–103]. Fig. 32 shows a simple example [100,101]. The output frequency is linearly related to the resistive unbalance of a Wheatstone bridge, while the duty-cycle is independently controlled by a second sensor. Resistors R_1–R_4 are the sensors while R_T represents the duty-cycle modulating element. Amplifiers A_1 and A_2 work, respectively, as

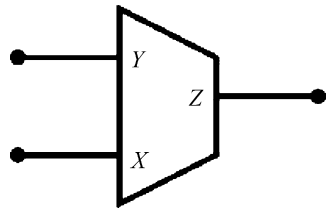

Fig. 33. Symbol for the second generation current conveyor (CC-II).

the integrator and the hysteresis comparator of the relaxation oscillator.

An improvement of the bridge sensitivity can be obtained by means of "active" bridges; for instance, an ISFET sensor and three MOSFET devices have been used in place of standard resistors [104,105].

Current-mode electronic interfaces for resistive sensors may take advantage of current conveyors; in particular, the second generation current conveyor (CC-II) [106,107] is a three terminals analog building block (see Fig. 33) which is described by the equations

$$\begin{cases} v_X = \alpha v_Y \\ i_Z = \beta i_X \end{cases} \tag{52}$$

where, ideally, α is equal to 1 and β may be equal to 1 or -1.

As an example, Fig. 34 shows the internal topology of an high performance CMOS CC-II [108]. Fig. 35 shows a CC-II-based resistive sensor interface [109] (the sensor is modeled by the resistance R_s). If the sensor resistance is

$$R_{\mathrm{S}} = R_{\mathrm{S0}}(1 + x) \tag{53}$$

where x is the relative sensor variation, the output voltage is

$$V_{\mathrm{OUT}} = \left(\frac{R_4 R_{\mathrm{s0}} V_{\mathrm{ref}}}{R_1 R_2}\right)x + \left(\frac{R_4 R_{\mathrm{s0}} V_{\mathrm{ref}}}{R_1 R_2} - \frac{R_4 V_{\mathrm{off}}}{R_3}\right) \tag{54}$$

The first term is linearly proportional to the relative resistance variation x; although dynamic techniques for the compensation of both the input offset and $1/f$ noise voltages would also be possible, the second term in (54) might allow to cancel the offset without reducing the speed of the interface (though, as with any other static technique, time-varying errors such as drift and $1/f$

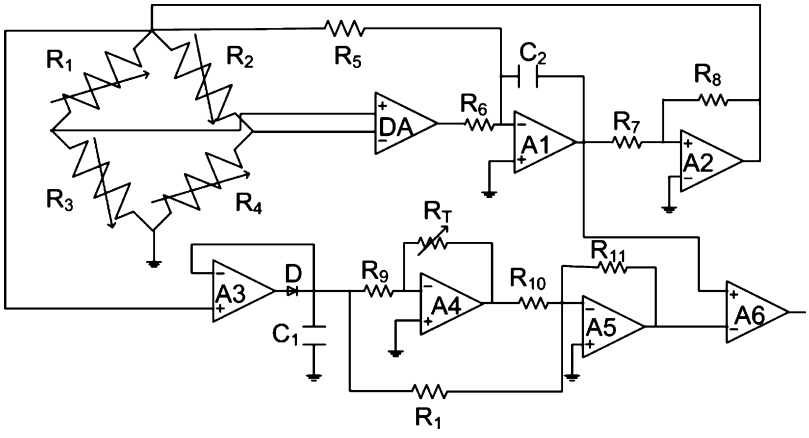

Fig. 32. A signal conditioning circuit for resistive sensors in bridge architecture.

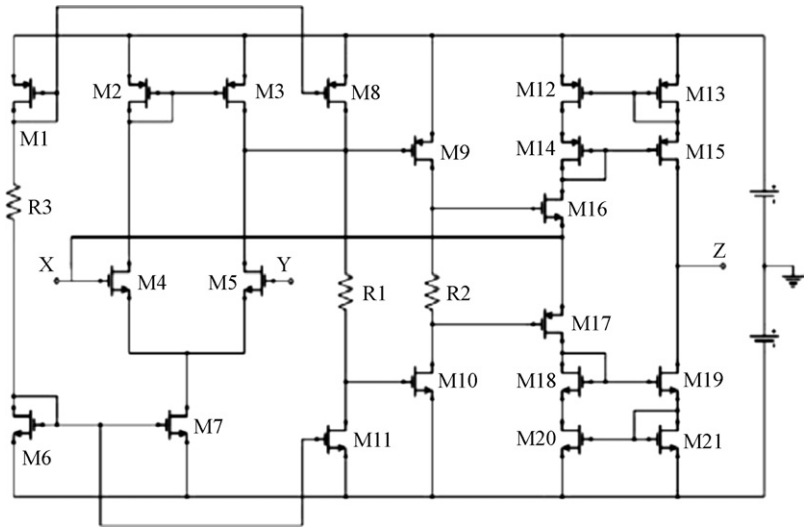

Fig. 34. High performance CMOS CC-II.

noise might not be compensated). This interface has been tested using the commercial AD-844 as the CCII and a supply voltage of ±10 V; the sensitivity of the resistance variation to voltage converter has been set to 0.18 V/kΩ, so that the output range is sufficient for resistances ranging from 25 to 90 kΩ. Fig. 36 shows the gas sensor response (output voltage versus time) for different H_2 gas concentrations (from 8 to 850 ppm). Being the overall noise (evaluated on a band of 1 MHz) equal to about 1 mV, the resistance resolution is lower than 6 Ω.

The interface has also been implemented in a CMOS system as shown in Fig. 37. In this case the sensitivity of the resistance variation to voltage converter is reduced to 16 mV/kΩ (because the supply voltages are 1.5 V, which are suitable for many low voltage low power applications).

The interfaces for resistive sensors which we have considered so far are only suitable for relatively small variations of the sensor resistances; however, in many practical cases the sensor resistances may change by orders of magnitude and/or the same interface must be used for the read-out of sensors with very different base-line resistances. A good strategy in these cases is to convert the resistance into a period (or, equivalently, into a frequency), so that scaling factors or high-resolution pico-ammeters are not required. A very simple interface which converts a resistive variation into a frequency is the bistable multivibrator shown in Fig. 38, which produces a square-wave waveform. Due to the limited speed of real op amps, the circuit is only suitable for relatively low frequencies (in the kilohertz

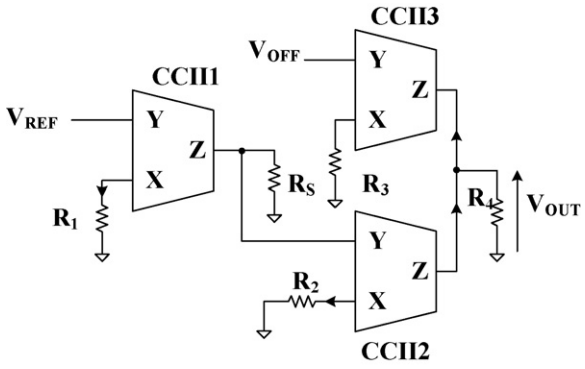

Fig. 35. CC-II-based interface for resistive sensors.

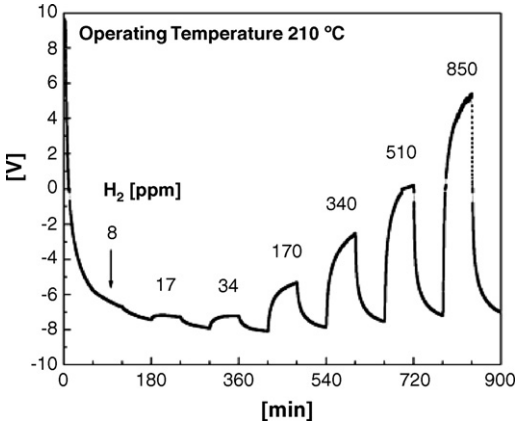

Fig. 36. AD844-based sensor interface output voltage vs. time.

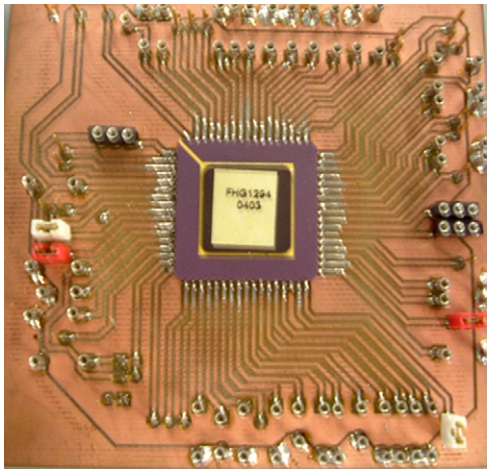

Fig. 37. CC-II-based sensor interface board.

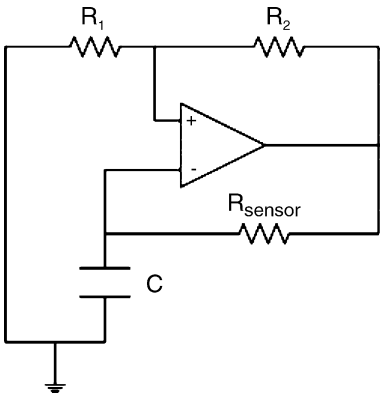

Fig. 38. Bistable multivibrator.

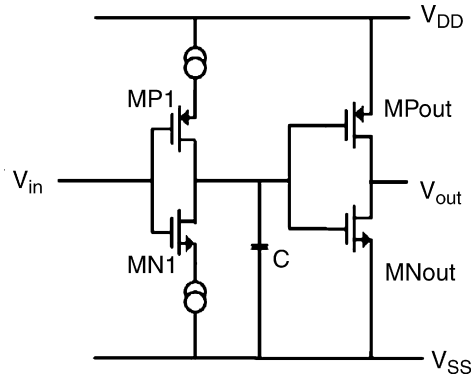

Fig. 39. Phase shifter.

range or lower); the capacitance value determines both the frequency range and the circuit sensitivity.

Phase shifters may also prove useful for the resistance-to-period conversion. For instance, the phase shifter shown in Fig. 39 [110] is a delay circuit which employs the capacitance C interposed between two inverter stages. If a square-wave input voltage V_{in} is applied at MP1 and MN1 gates, the capacitor C is charged and discharged with a ramp-type behaviour. The output voltage is a square-wave delayed with respect to the input by

$$T_D = \frac{(V_{DD} - V_{SS})C}{2I} \tag{55}$$

where I is the biasing current. Fig. 40 shows an interface which uses this phase-shifter for implementing an oscillator.

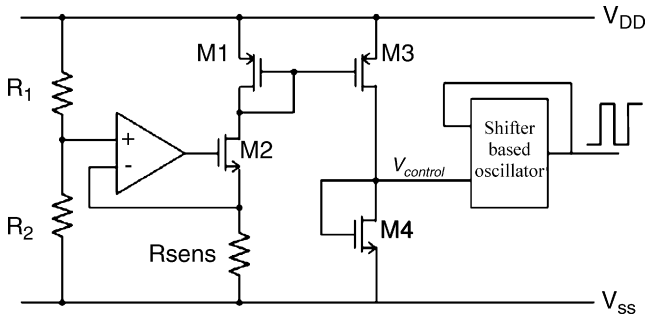

Fig. 40. Resistive sensor interface based on phase shifter.

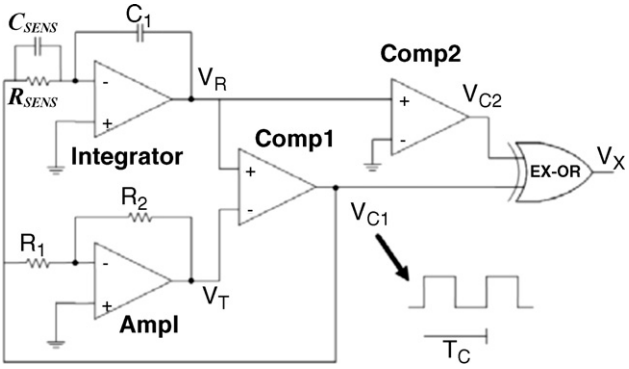

Fig. 41. Wide-range resistive sensor interface with parasitic capacitance estimation.

If the control voltage $V_{control}$ properly determines the biasing current of the phase shifter, the delay time becomes

$$T_D = \frac{R_1 + R_2}{R_2} C R_{sens} \left(1 \pm \frac{R_1 + R_2}{R_2} \frac{|V_{OS}|}{V_{DD} - V_{SS}}\right) \tag{56}$$

where V_{OS} is the input offset voltage of the op amp. Connecting the input and the output nodes of the phase shifter as in Fig. 40, the oscillation period is

$$T_{osc} \cong 2 \frac{R_1 + R_2}{R_2} C R_{sens} \tag{57}$$

which depends on the sensor resistance R_{sens}. In this case, the resistances R_1 and R_2 determine the circuit sensitivity.

Figs. 41 and 42 show the schematic and the prototype of an improved resistance-to-frequency converter [111,112]. This circuit works for high dynamic range (DR) resistive sensor measurements and is able to estimate, with very high precision and excellent linearity, the sensor resistance R_{sens} over seven orders of magnitude, and, eventually, the parasitic capacitance C_{sens} of the sensor.

The circuit is constituted by two comparators, an inverting integrator, an inverting amplifier and an EX-OR digital logic block. Fig. 43 shows the voltage signals at the different nodes of the interface; the first comparator (Comp 1) generates a square-

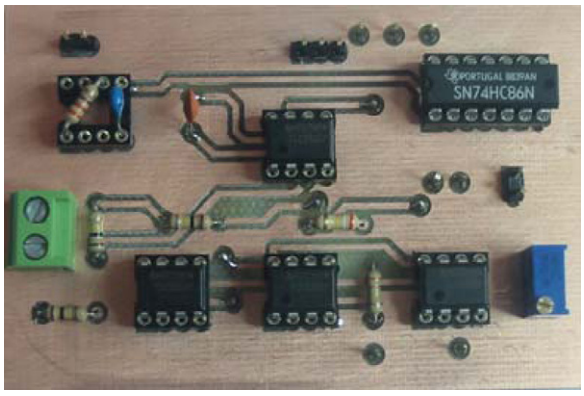

Fig. 42. Prototype of the circuit shown in Fig. 41.

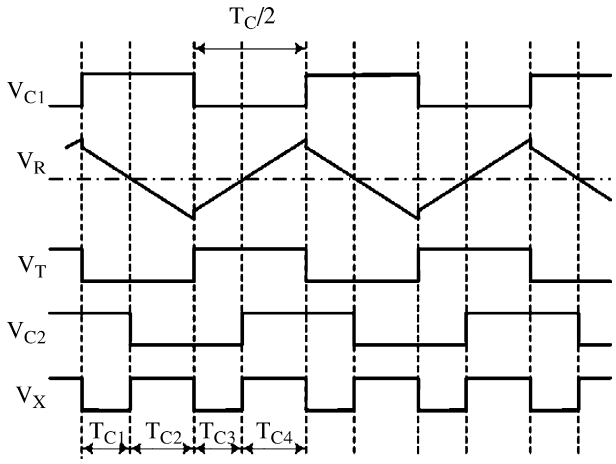

Fig. 43. Voltage levels generated by each block of the interface.

wave signal with an oscillating period

$$T = 4GC_1R_{\mathrm{SENS}}\left(1 - \left(\frac{C_{\mathrm{SENS}}}{GC_1}\right)\right) \tag{58}$$

which is linear with the sensor resistance.

In this circuit low offset, high slew-rate amplifiers are needed for keeping small the measurement errors [111]. If the product $G \times C_1$ is much higher than the parasitic capacitance C_{sens}, the period may be approximated as follows

$$T = 4GC_1R_{\mathrm{SENS}} \tag{59}$$

The EX-OR gate generates a square-wave signal, whose duty-cycle depends on C_{SENS}. It is therefore possible to estimate the parasitic sensor capacitance, through the second comparator and the EX-OR gate, according to the following expressions:

$$C_{\mathrm{sens}} = G \times C_1 \times \frac{T_{C2} + T_{C4} - T_{C1} - T_{C3}}{2T_{C2} + 2T_{C4}},$$
$$R_{\mathrm{sens}} = \frac{T_{C2} + T_{C4}}{2GC_1} \tag{60}$$

In some applications, traditional resistance-to-period conversion strategies are not acceptable, For instance, a smart device for environmental monitoring contains an array of sensors and a digital system which must perform complex data processing tasks (e.g. by means of a dedicated pattern recognition software) in order to detect the target gases and extract their concentration [113–115]. The base-line resistances of the sensors may typically vary from a small value (i.e. 200 Ω) up to a very big one (i.e. 10 MΩ); furthermore, the sensor resistance must be measured with a precision near to 0.1% in order to detect the different gasses with a sufficient resolution (i.e. 1 ppm). These constraints would require, without any range compression, a linear front-end circuit with an impractical resolution (for a low cost implementation). Although an oscillator with a period related to the sensor impedance would solve this problem, it would be too slow. Another solution could be a compression for the R_{sens} value; unfortunately, even if wide range is guaranteed by this technique, it is difficult to get an accuracy better than 1% [116,117]. Fig. 44 shows an alternative interface which, after calibration, grants a final worst case measurement with a precision (verified testing the silicon device) better than 0.1% in about 10 ms per sensor query, fast enough for allowing dynamic pattern recognition algorithms, which gather important information from the derivatives of the sensor responses. The desired resolution all over the required dynamic range has been satisfied by splitting the system scale in 10 sub-intervals, each of them with an operative width of about half decade. Calibration has been used to compensate the offset and gain error mismatch by means of two DACS which regulate, respectively, a programmable current sunk from virtual ground of the amplifier (for the offset error) and sensor bias voltage V_{REF} (for the gain error).

Fig. 45 shows the photograph of the sensor and Fig. 46 shows the microphotograph of the realized electronic interface chip [118–120]. The device has been characterized over the whole dynamic range, first, by testing separately every single one of the 10 partially overlapped scales and, then, by re-building the over 5 decades information correcting inter-scale offset and gain error mismatch. The relative error in the resistance value measurement, always performed over the complete 5.3 decades dynamic

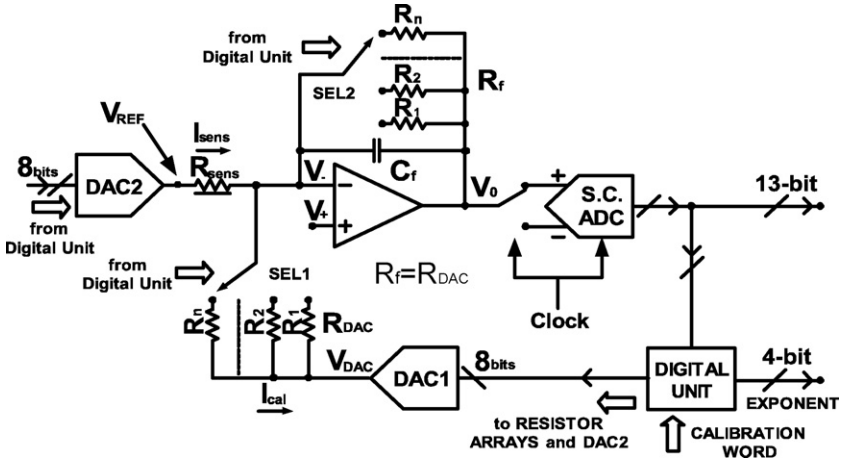

Fig. 44. Block diagram of the interface circuit.

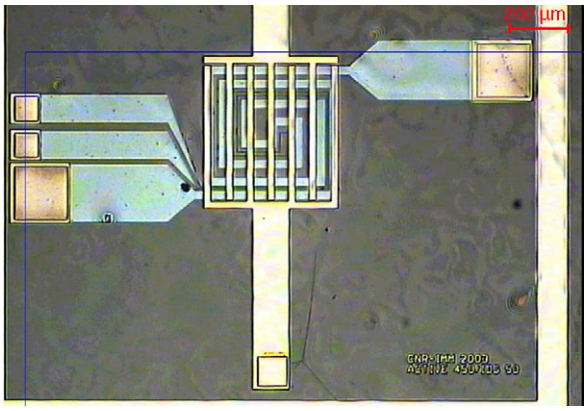

Fig. 45. Microphotograph of the chemical sensor.

range, is shown in Fig. 47. Relative tested root mean square error for R_{sens} value measurement is 0.024%. A typical ethanol concentration measurement realized with the described micromodule is shown in Fig. 48.

8.2. Thermal ΣΔ modulation for temperature control

As many physical, chemical, and biological quantities depend on temperature, temperature regulation is often necessary in sensors systems. An automatic temperature regulation system must comprise a temperature sensor, a thermal actuator and an electronic interface. As to the temperature sensor, there are several possibilities (e.g. temperature dependent resistors, bipolar junction transistors, etc.); in standard integrated circuits, in most practical applications, it is convenient to take advantage of the temperature dependence of the base to emitter voltage of bipolar junction transistors [39,46–48]. As to the actuators, if simplicity and low cost are main issues, "heating actuators" are far

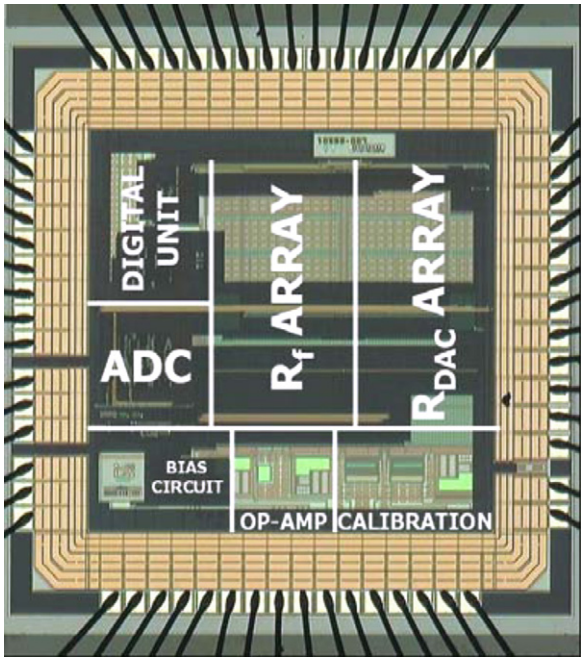

Fig. 46. Microphotograph of the electronic interface circuit chip.

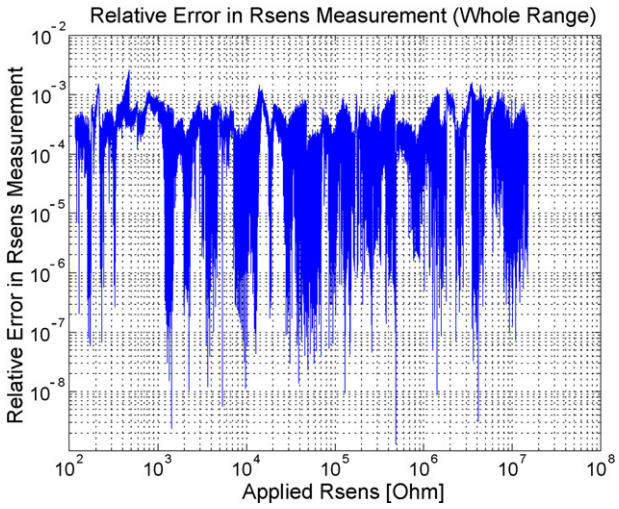

Fig. 47. Relative error of R_{sens} measurement [100–20 MΩ].

more practical than "cooling actuators" because any electronic device where power losses occur is an heater (e.g. resistors or transistors). In some cases the same resistor may be used both as a temperature sensor and as an actuator (e.g. in hot-wire anemometers, which use King's law for estimating the flow velocity [121,122]). Recently, it has been shown that in various applications the so called thermal ΣΔ modulation (which was originally introduced for integrated flow sensors [121]) is a very simple and effective strategy for temperature regulation [123–125]; the basic principle of thermal ΣΔ modulation is schematically illustrated in Fig. 49; the comparator compares the output voltages of two temperature sensors (TS_1 and TS_2) which are in thermal contact with, respectively, the object whose temperature must be regulated and with the environment. Depending on the output of the comparator, the D type flip-flop enables or disables the heater. The equivalent electric low pass filter (R_{TH}, C_{TH}) models the thermal system (see Fig. 4) and acts as the integrator in the ΣΔ modulator (noise shaping). The desired

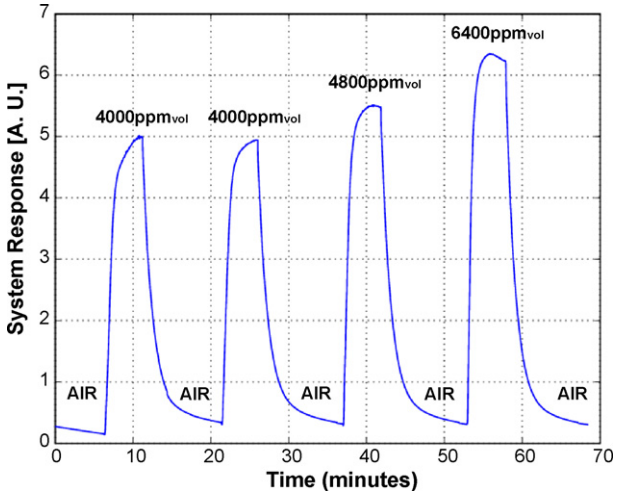

Fig. 48. Typical response of resistive gas sensors exposed to different ethanol concentrations obtained with the integrated interface shown in Fig. 46.

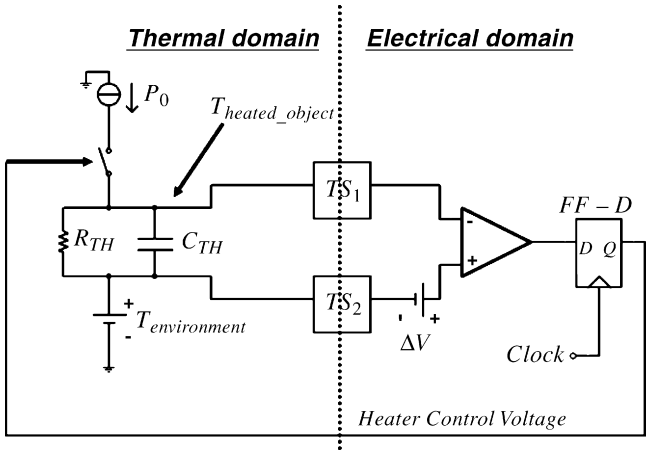

Fig. 49. Thermal $\Sigma\Delta$ modulation (basic principle).

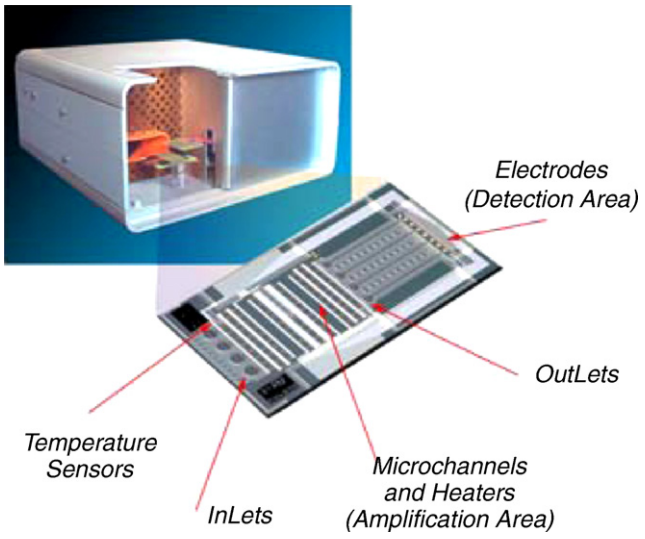

Fig. 50. The ST DNA chip and a prototype of the temperature control system.

temperature may be fixed by properly selecting the voltage ΔV; the flow velocity may be deduced from the (digital) output of the flip-flop.

As a first example, the standard method for DNA amplification (polymerase chain reaction, PCR) requires that a given DNA sequence is passed through proper thermal cycles. Nowadays the PCR is generally done by using macroscopic systems so that relatively large amounts of reagents and long analysis times are necessary. The costs may be strongly reduced by integrating the whole system within a single chip (Lab-on-Chip or DNA chip) [126]; clearly, the DNA amplification requires that the temperature of the chip be properly controlled. Here we describe a low cost user-friendly system [123] for the temperature control of the ST Microelectronics Lab-on-Chip (an industrialized version of this prototype is now commercialized by ST Microelectronics).

The ST DNA chip comprises integrated microchannels, resistive temperature sensors, heaters (resistors) and electrodes (required for the DNA detection), as shown in Fig. 50 (which also contains a photo of the first prototype of the temperature control system). Although in principle the electronic circuitry for the temperature control could be integrated on the chip itself, this would significantly increase the costs of the special process for fabricating the microchannels. An external temperature control system is therefore necessary for the read-out of the temperature sensors and for driving the heating and cooling actuators; the maximum allowed temperature error is $\pm 0.5\,^{\circ}C$; both the cooling and the heating rates must be larger than $10\,^{\circ}C/s$. The complete temperature control system must be connected to a PC by means of a ST7 microcontroller (see Fig. 51); the user may set the temperature and the duration of each step. In order to reduce the analysis time, the heating and the cooling should be as fast as possible; since the on-chip heaters may be supplied by large voltages, the heating may be very fast; on the contrary passive cooling would be too slow and some kind of active cooling (e.g. a fan) is necessary. In order to obtain the required accuracy, the sensors resistances are read out using a four-wires measurement. The inaccuracies of the current and voltage references used for the temperature measurement are compensated by comparing the sensors resistances and a high-accuracy resistor; this comparison automatically implements an autozero technique. A single, high quality differential analog to digital converter rejects the common mode disturbances; this is, however, not enough due to the extremely large currents (the peak currents are above 1 A) which drive the heaters and the fan, so that a careful layout is also necessary for keeping low the temperature measurement errors.

Fig. 52 shows some thermal cycles; the three temperatures correspond to annealing, synthesizing, and denaturation. Fig. 53 shows the temperatures measured in two different points of the

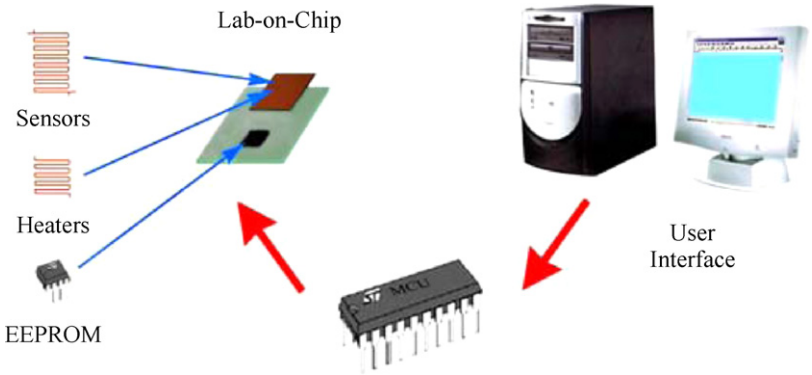

Fig. 51. High level description of the temperature control system.

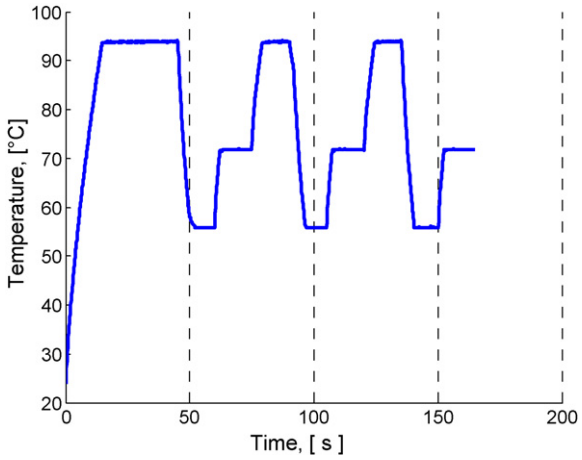

Fig. 52. Thermal cycles.

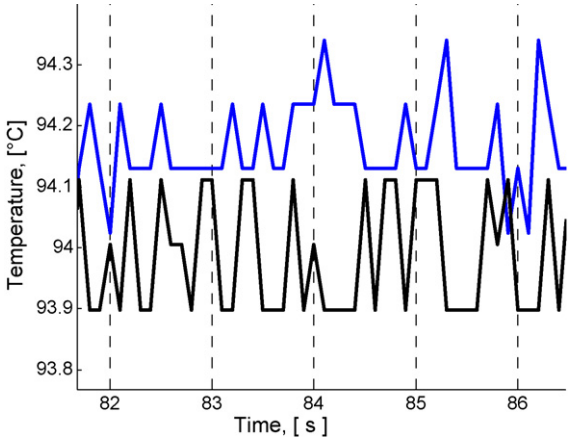

Fig. 53. Estimated temperatures in different points of the DNA chip with a nominal temperature equal to 94 °C; the temperature error is within the specs.

Lab-on-Chip with a nominal temperature equal to 94 °C; the temperature error is within the specs. Fig. 54 shows an heating rate above 10 °C/s. High cooling rates (up to 20 °C/s) may be obtained by using an air compressor; a fan allows to achieve cooling rates in the order of 10 °C/s (see Fig. 55).

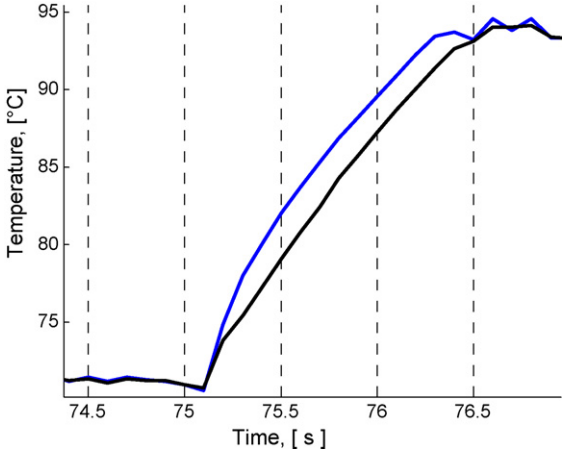

Fig. 54. Heating. Using a supply voltage equal to 12 V a heating rate above 10 °C/s may be easily obtained.

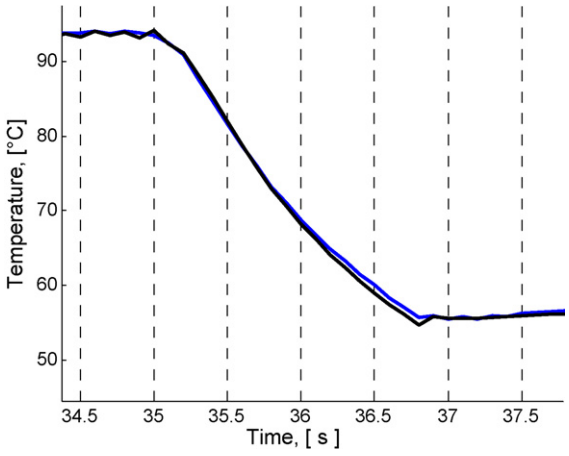

Fig. 55. Cooling. High cooling rates (up to 20 °C/s) may be obtained using an air compressor; a fan allows to achieve cooling rates in the order of 10 °C/s.

As another example, quartz microbalances (QMBs) are widely used as resonating sensors; since QMBs have significant cross-sensitivities toward the temperature, some sort of temperature regulation is generally necessary. The traditional approach for controlling the temperature of QMBs requires controlling the temperature of the chamber where QMBs are inserted; clearly, this method is rather inaccurate, slow, power inefficient, and not flexible. In fact, first, the thermal contact between microbalances and the gas chamber may not be satisfactory; second, the thermal time constant of the gas chamber may be much larger than the thermal time constant of the microbalance; third, the thermal mass of the gas chamber is much larger than the thermal mass of the microbalances; fourth, it is not possible to set different temperatures for different microbalances. All these issues may be solved by employing the modified quartz microbalance shown in Fig. 56 [124]; here an auxiliary terminal allows the top electrode to be used as a resistor; the resistor acts as a temperature sensor which is, first, in good thermal contact with the microbalance and, second, is characterized by a very small thermal mass. The same resistor is also used as the heater (hot-wire anemometer). In comparison with traditional solutions, this approach is more accurate, faster, cheaper, more flexible, and more power efficient. In order to take full advantage of the slightly modified quartz microbalance, a $\Sigma\Delta$

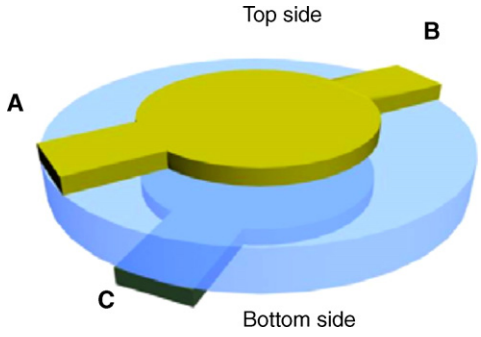

Fig. 56. Quartz crystal with an auxiliary terminal (B). The electrodes are constituted by a gold/chromium film whose thickness is about 1500 Å. The gold/chromium top electrode is used as a temperature sensor, heater, flow sensor and electrical contact for the resonator.

electronic interface may be used so that the QMB contemporarily acts as temperature sensor, flow sensor, heater, and resonator [124]; there is no detectable interference between the oscillator circuit and the $\Sigma\Delta$ interface. It should be mentioned that, as a unique advantage of this approach, the flow velocity is automatically measured by the QMB sensor itself; this is important as QMBs often show significant cross-sensitivities toward the flow velocity.

The simple circuit depicted in Fig. 57 constitutes the $\Sigma\Delta$ electronic interface: the feedback loop equates the ratios R_A/R_B and R_{REF}/R_{Heater}; after calibration, this corresponds to keep the microbalance at a desired temperature. In practice, if $V_{S1} > V_{S2}$, the output of the comparator is low and, therefore, M_1 is switched on by the flip-flop D, thus heating the quartz, so that R_{Heater} increases (metal resistors have positive temperature coefficients). On the contrary, if $V_{S1} < V_{S2}$, the output of the comparator is high and, therefore, M1 is switched off by the flip-flop D. The resistance R_{AUX} allows both a reliable start up and a reliable comparison (between V_{S1} and V_{S2}) when M_1 is off. Although this solution is extremely simple, an important trade-off exists. On the one hand, a non-zero current will flow through the top electrode even when M_1 is off and no heating is desired; in order to keep this current small R_{AUX} must be enough large. On the other hand, when M_1 is off, an accurate comparison between the voltages V_{S1} and V_{S2} requires that R_{AUX} be enough small. In practice this is not an issue for some applications; eventually, this trade-off may be eliminated by patterning two different resistors (temperature sensor and heater) on the top electrode of the QMB (this, however, requires at least an additional auxiliary terminal). Fig. 58 shows the output voltage of a thermocouple which has been placed in good thermal contact with the quartz microbalance when different temperatures are set by the temperature control system (the slow response is due to the low pass filter of the circuitry for the read-out of the thermocouple; the speed response of the temperature control system may be accurately simulated by means of an appropriate equivalent electric circuit [124]).

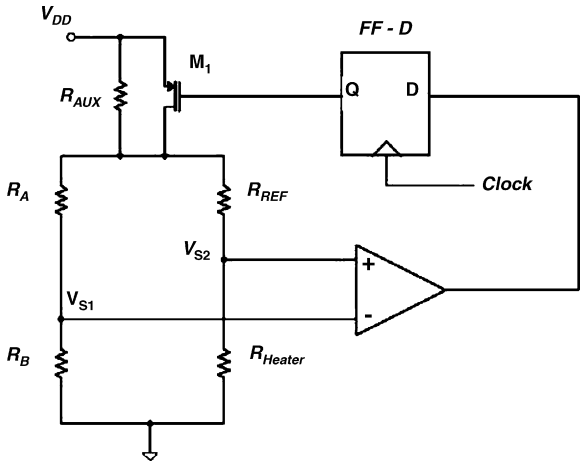

Fig. 57. $\Sigma\Delta$ interface for the hot-wire anemometer. The (digital) output of the FF-D is related to the flow speed.

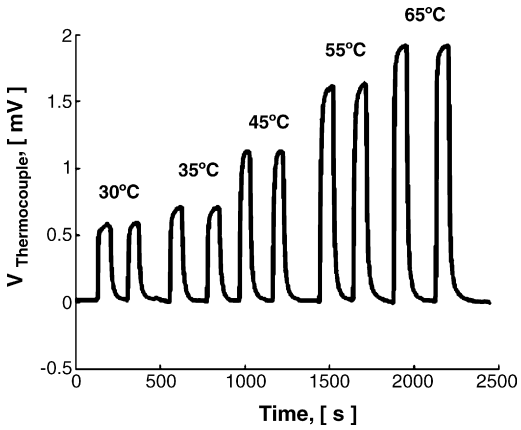

Fig. 58. Thermocouple output voltage; the thermocouple is in thermal contact with the quartz microbalance.

8.3. Fluxgate magnetic sensor

New methods and devices for the magnetic field measurement either for electrical instrumentation or compass devices have been proposed in recent years. New topologies of planar integrated micro-fluxgate [127,128] have been presented, which allow small dimensions and low power consumption. Developments are expected especially in terms of new processes for the deposition of the magnetic core. A solution to realize the fluxgate magnetic sensors could be the RF magnetron sputtering, which allows to create very thin magnetic cores (about few micron) with suitable magnetic properties. A magnetic material with both small geometrical dimensions and high magnetic permeability is the key issue to achieve magnetic sensors with low power consumption. On the other hand, standard CMOS technologies have already demonstrated their potential for implementing low power and small area devices, and for interfacing standard magnetometers (usually realized on PCB structures [129]) or other sensors, such as gyroscopes or accelerometers. An important goal is to combine the benefits of both technologies for the fabrication of a planar magnetometer, depositing the ferromagnetic material on top of the electronics (on the same die). In order to compete with classical magnetometers, the integrated devices must have comparable performance, in addition to the main features of standard IC products.

In order to take full advantage of this approach (low power consumption and small area occupation), an integrated CMOS front-end circuit is necessary; although for our application a microsystem approach has been preferable, this CMOS circuit would also be useful for the micromodule approach. Indeed, if the magnetic sensors previously mentioned will be realized in a separate die it is quite easy to bond together the dies and attach them on the same substrate. In literature, front-end circuits for fluxgate sensors are typically based on a sinusoidal or pulsed excitation [130].

The approach adopted in the proposed circuit, instead, exploits a triangular current to feed the excitation coil and a synchronous demodulation for reading out the voltage induced in the sensing coils. This solution represents a trade-off between the low-noise performance achieved with sinusoidal excitations

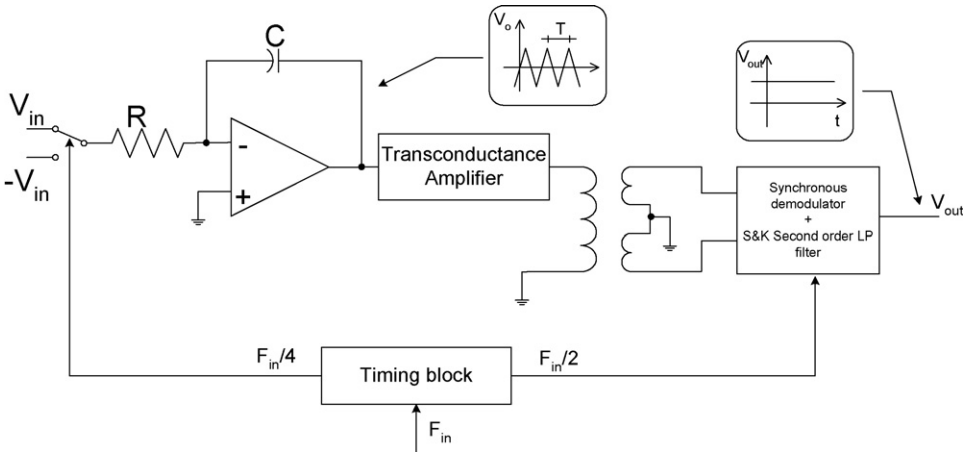

Fig. 59. Block diagram of the complete microsystem for magnetic field sensing.

and the simple implementation of solutions based on pulsed excitation [131]. The front-end circuit can be divided in three main blocks: the timing block, the excitation block and the read-out unit. The timing block is common to the other two and provides the synchronization of the entire system. The block diagram of the entire microsystem is shown in Fig. 59. The circuit has been realized in a standard 0.35 μm CMOS process, with two poly, four metals, 5 V devices and high resistivity polysilicon [132,133].

Photographs of the chips containing the sensor and the read-out circuit are shown in Figs. 60 and 61, respectively.

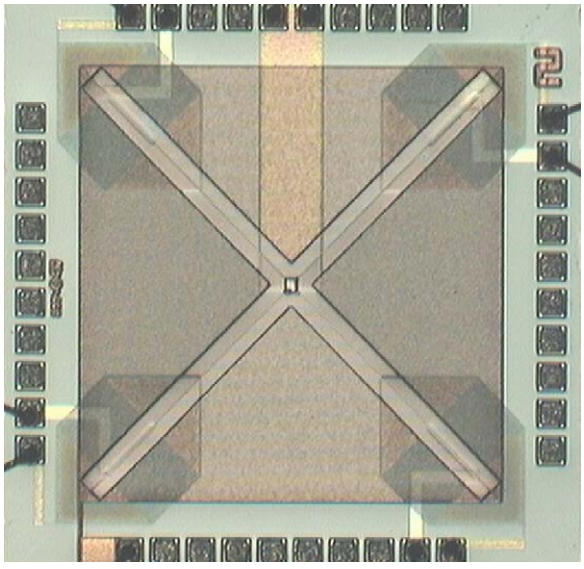

Fig. 60. Microphotograph of the magnetic sensor chip.

Fig. 61. Microphotograph of the electronic interface circuit chip.

A typical measurement obtained rotating the sensor in the Earth magnetic field is shown in Fig. 62.

8.4. Biaxial accelerometer

Single-axis linear accelerometers are widely used. However, a number of recently developed applications require biaxial accelerometers, which detect the acceleration in two orthogonal axes (i.e. on *x*- and *y*-axis). All of these applications are characterized by similar specifications and, in particular, small bandwidth (in the order of few tens of hertz) and high sensitivity. The considered biaxial accelerometer is composed of a biaxial linear acceleration sensor and an electronic interface circuit included in the same package.

The biaxial acceleration sensor is realized with silicon micromachined MEMS technology and uses a single proof mass to detect the acceleration in both the *x* and *y* directions. The device realized with this technique is efficient because it provides a very accurate 90° angle between the two linear sensors, thus

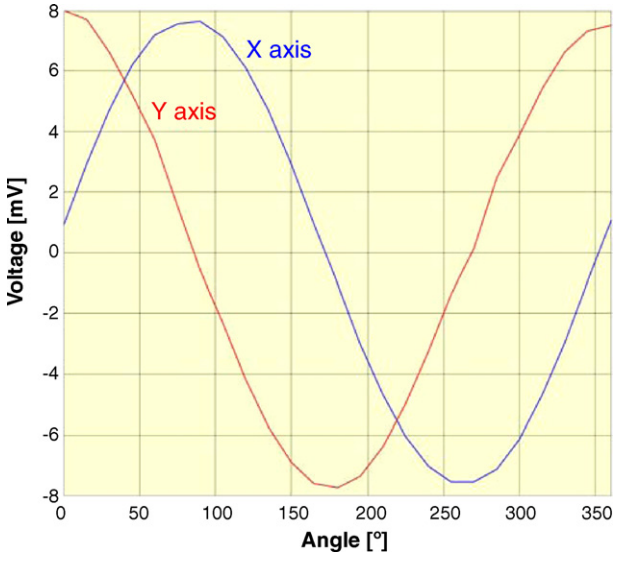

Fig. 62. Typical measurement obtained rotating the magnetic sensor in the Earth magnetic field.

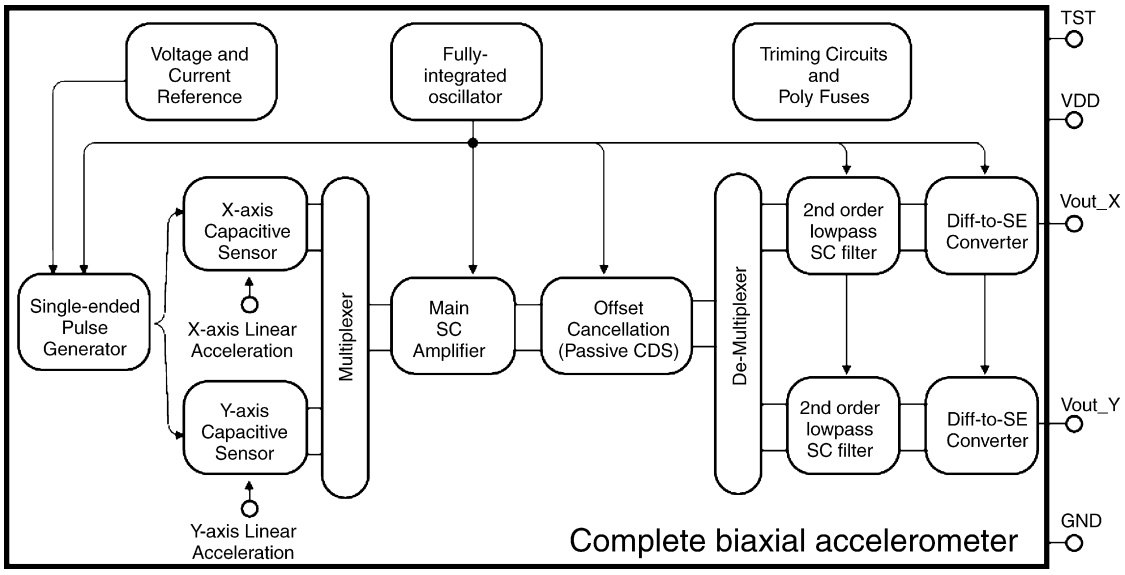

Fig. 63. Overall system architecture of the biaxial accelerometer.

allowing better performance in comparison with devices based on two separate single-axis sensors.

The micromodule approach allows to separately optimize the sensor and the interface since they can be realized in different technologies. The use of a single technology typically results in stringent trade-offs in the design of sensor and electronics. On the other hand, the cost of the choice of using different technologies is the larger parasitic input capacitance, which requires higher power consumption to reach the same dynamic range. The above considerations motivate the higher power consumption of this device realized with a two-chip solution in comparison with single-chip solutions.

The overall block diagram of the proposed biaxial linear accelerometer is shown in Fig. 63. The processing channel consists of: a biaxial acceleration sensor, which is driven by a voltage reference and drives a main switched-capacitor amplifier (MSCA). The output of the MSCA is fed into a low pass SC filter whose differential output is converted to single-ended one with an instrumentation amplifier block. All the operations are controlled by clock phases generated by an on-chip oscillator. For the overall processing chain, an open loop architecture has been used since it allows a large dynamic range to be achieved even in presence of a lossy sensor.

The biaxial MEMS-based sensor is a surface micromachined based polysilicon structure implemented in a process called THick Epitaxial Layer for Micromotors and Accelerometers (THELMA) [134,135], specifically developed for the realization of inertial sensors (angular, linear accelerometers and gyroscopes).

The equivalent electrical circuit of the biaxial sensor is shown in Fig. 64. The true sensor capacitances (whose variations have to be measured) are C_{s1x} and C_{s2x} for the x-axis, and C_{s1y} and C_{s2y} for the y-axis. All the other impedances in the scheme are parasitic elements in the MEMS-based sensor implementation. When a linear acceleration is applied to the sensor, the proof mass displaces from its nominal position, causing an imbalance in the sensor capacitive half-bridges of C_{s1x} and C_{s2x} for the x-axis, and of C_{s1y} and C_{s2y} for the y-axis. The interface circuit chip translates these minimal capacitance changes into calibrated analog voltages at the output pin proportional to the proof mass movement, and hence to the applied acceleration.

The capacitive imbalance is measured using charge integration [136,137] in response to a fixed voltage pulse applied to the sense capacitors. The interface circuit can then be implemented by using switched-capacitor techniques. The complete signal processing chain uses a fully differential structure to improve system performance robustness. The unbalanced sensor capaci-

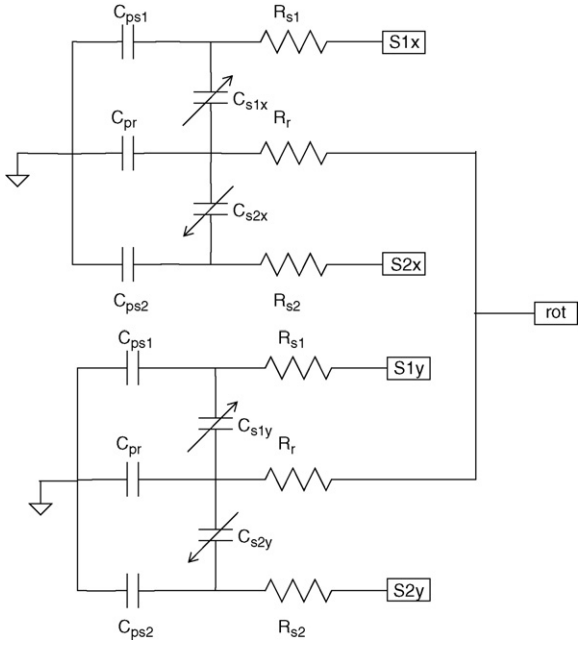

Fig. 64. Equivalent electrical circuit of the biaxial sensor.

tance features a full-scale (FS) signal value (for a ±1 g full-scale acceleration) of ±10 fF. This is superimposed to a DC-value for C_{s1x}, C_{s2x}, C_{s1y}, and C_{s2y} of about 1 pF. A single pulse waveform is applied to both capacitors of the sensor in order to avoid mismatches. The reference voltages control the amplitude of the applied pulse. The resulting charge is injected into the virtual ground of the MSCA. This block has very stringent requirements in terms of noise, which can be satisfied using large input devices and a high input stage current level. This results in the main contribution to the total area and power consumption. To reduce this contribution, we have to use a single MSCA, which is time shared between the two (*x*-axis and *y*-axis) measurement chains, as shown in Fig. 63. Notice that since a single proof mass is used for both *x*- and *y*-axes acceleration measurement, when the measurement on an axis is active, the measurement on the other axis has to be disabled. This makes useless a read-out architecture with one MSCA for each axis. The multiplexer (MUX) and the demultiplexer (DEMUX) in the scheme are implemented in the digital part by producing suitable driving signals for the switches and not using additional series switch which could be detrimental for the system performance. The offset and 1/*f* noise of the MSCA is also cancelled through the only-passive correlated-double-sampling (CDS) structure implemented at its output nodes. This solution has been preferred to other ones implemented at the operational amplifier input nodes due to its higher robustness with respect to parasitic capacitance and charge injection.

The fully integrated switched capacitor filter (SCF) implements a 30 Hz cut-off frequency with only 0.6 mm^2 of capacitor area. In other solutions, this filtering is implemented with external RC filters increasing costs and external components count. In addition, the SCFs guarantee the accuracy of the transfer function, which allows optimizing the chain performance in order to slightly increase the chain resolution.

Regarding the architecture of the system, the SCFs have not been included in the time-shared section because their output samples have to be continuously available for the following continuous-time differential-to-single-ended converter. In the case of using a single time-shared SCF, the SCF output should have to be sampled and held with two S&H blocks. Therefore, no considerable power consumption and area saving would be achieved. In addition, the single SCF should operate with a double sampling frequency, increasing the power consumption.

The complete device in standard operation needs only five pins (VDD, GND, Out-X, Out-Y, and a pin for testing purpose). This is possible thanks to the on-chip generation of reference voltages/currents and of the reference frequency. The overall device reference voltages are generated on chip using a resistive string connected between the supply rails. This ratiometric solution reduces the dependence of the performance from temperature. A fully integrated oscillator whose nominal resonance frequency is 1 MHz generates the reference clock for the entire device. From the output waveform proper clock phases for the MSCA and for the SCF are obtained.

The electronic interface circuit has been fabricated in a 0.5 μm CMOS technology, resulting in a die size of (2.60 mm × 2.84 mm). From a single 5 V supply it consumes 45 mW.

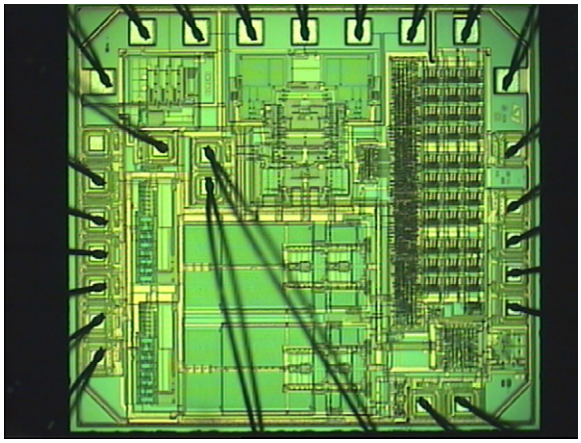

Fig. 65. Microphotograph of the electronic interface circuit chip for the biaxial accelerometer.

Fig. 65 shows the electronic interface circuit chip microphotograph [138]. The interface circuit (on the right hand side) is assembled with the biaxial mechanical sensor (on the left hand side) in a standard SO24 plastic package, as shown in Fig. 66.

The measurements have been performed on a linear shaker controlled by a personal computer running the evaluation software. A reference commercial linear accelerometer was used to calibrate the system. The characterization software was performing the measurements on all the relevant device parameters. In addition, all the trimming procedures have been implemented and all the data were collected before and after the poly-fuses trimming process. The device is able to measure acceleration in the range [−1 g, +1 g], which corresponds to a full-scale of 2 g. The output noise floor is about 26.1($\mu g/\sqrt{Hz}$), which corresponds to a total output noise of 200 μg. The two main parameters of the device are the sensitivity and the ratio between the full-scale and the minimum detectable signal (mDS). These parameters for several samples are plotted in Fig. 67a and b, respectively. The parameters appear to be centered on the mean values of 2 V/g for the sensitivity and of 80 dB for the ratio

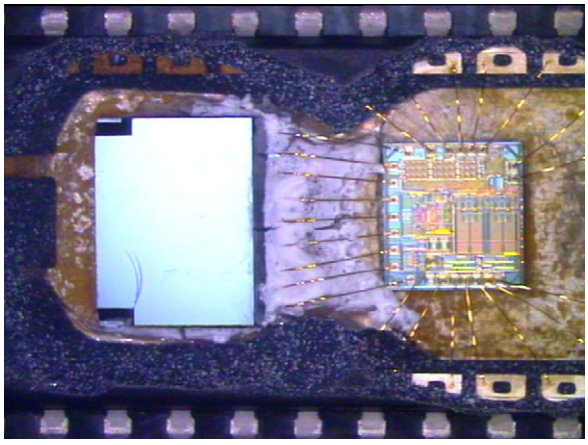

Fig. 66. The two-chip biaxial accelerometer micromodule.

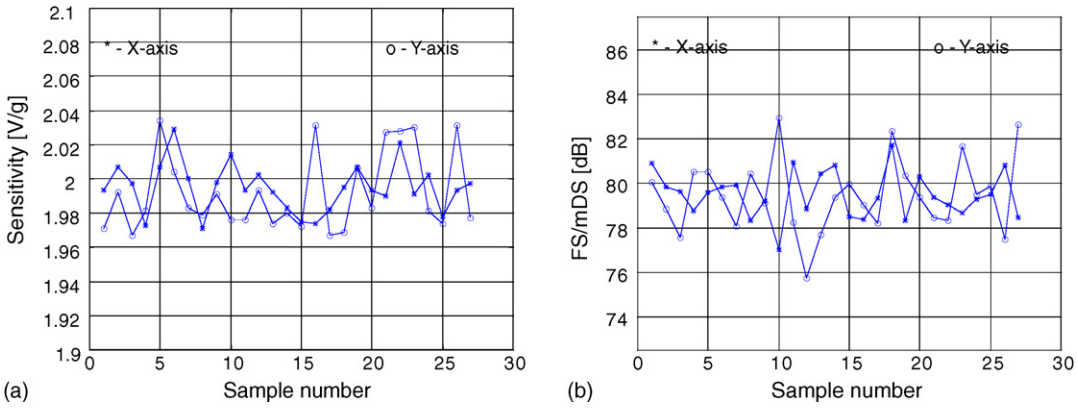

Fig. 67. (a) Device sensitivity and (b) DR for several samples of the biaxial accelerometer.

FS/mDS. In addition, the distribution of sensitivities is showing a spread, which is less than 2.5%. This corresponds to a minimum detectable capacitive change of about 2 aF.

8.5. Oscillators

Resonating sensors are widely used in a variety of measurement systems [139–149]. The most accurate way for extracting information from a resonating sensor is to measure its impedance as a function of the frequency; this kind of measurement traditionally requires a bulky and expensive network analyzer. Although it has been shown that the impedance of a resonator can be analyzed (at frequencies close to the resonant frequencies) by means of a system using a variable frequency (voltage controlled) oscillator [141], it is still too complex and expensive for most applications. A convenient solution in such cases is to include the resonator as a part of an oscillator and to use the oscillating frequency as the sensor output signal. In comparison with high performance resonators for oscillators, resonating sensors typically have a much lower Q; in fact, in order to achieve a high sensitivity, resonating sensors with higher oscillating frequencies are generally preferred (though they have lower Q values); moreover, some types of coating significantly reduce the Q of the resonator; in some cases the resonator may even be in contact with liquids [142–145], resulting in very low Q.

The reduced Q of a resonator potentially makes the oscillating frequency of the complete oscillator more sensitive to circuit parameters and interfering signals such as the temperature and the supply voltage. In practical oscillators, for the oscillations to build up, there must be two poles of the system, at the start up phase, with a positive real part; this condition leads to oscillations whose amplitude increases with time; if there is no automatic gain control, the amplitude of the oscillations will be limited by the non linearities of the circuit. Since, in general, non linearities may exhibit a complex dependence on both the supply voltage and the temperature, some sort of automatic gain control is often employed [150,151].

A simple circuit for resonating sensor is the three points oscillator shown in Fig. 68 (dynamic circuit). If, according to the Butterworth-Van Dyke model, we approximate the resonator by means of the shunt connection of a capacitance C_P and of a series RLC resonator (R_S, L_S, C_S), assuming an ideal automatic gain control circuitry, and using the useful approximations proposed in [150], the g_m value may be found as follows

$$\begin{aligned} &\alpha = C_P^2 C_{12}^2 R_S, \qquad \beta = -C_1 C_2 C_{12}^2, \\ &\gamma = \omega_S^2 C_1^2 C_2^2 (C_P + C_{12})^2 R_S \\ &\qquad\qquad \Downarrow \\ &g_m = \frac{-\beta - \sqrt{\beta - 4\alpha\gamma}}{2\alpha} \end{aligned} \tag{61}$$

so that the oscillating frequency will be [152,153]

$$\begin{aligned} f_0 &= \frac{1}{2\pi}\left(\frac{-Y}{2L_S} + \sqrt{\frac{Y^2}{4L_S^2} + \frac{1}{L_S C_S}}\right), \\ Y &= \mathrm{Im}[z_{CX}(f_S) \\ &= \left(\frac{-1}{2\pi f_S}\right) \frac{[g_m^2 C_{12}^2 C_P + \omega_S^2 C_1^2 C_2^2 (C_P + C_{12})]}{[g_m^2 C_P C_{12}^2 + \omega_S^2 C_1^2 C_2^2 (C_P + C_{12})^2]} \end{aligned} \tag{62}$$

where

$$C_{12} = \mathrm{series}(C_1, C_2) = \frac{C_1 C_2}{C_1 + C_2} \tag{63}$$

From this expression it is clear that, even with an ideal circuit for automatic gain control, the oscillating frequency does not depend only on the parameters of the resonating sensors. For this reason, in some applications, different approaches may be preferable. As an example, Fig. 69 shows a PTAT oscillator [153]; in this circuit the existence of non linear phenomena is accepted (no automatic gain control is employed), but a proper

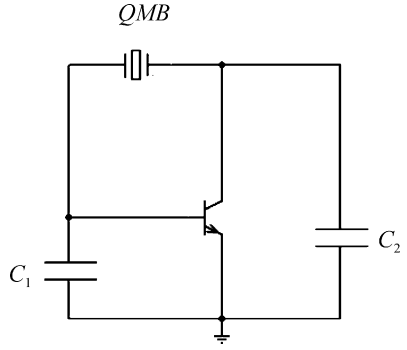

Fig. 68. Three point oscillator (dynamic circuit).

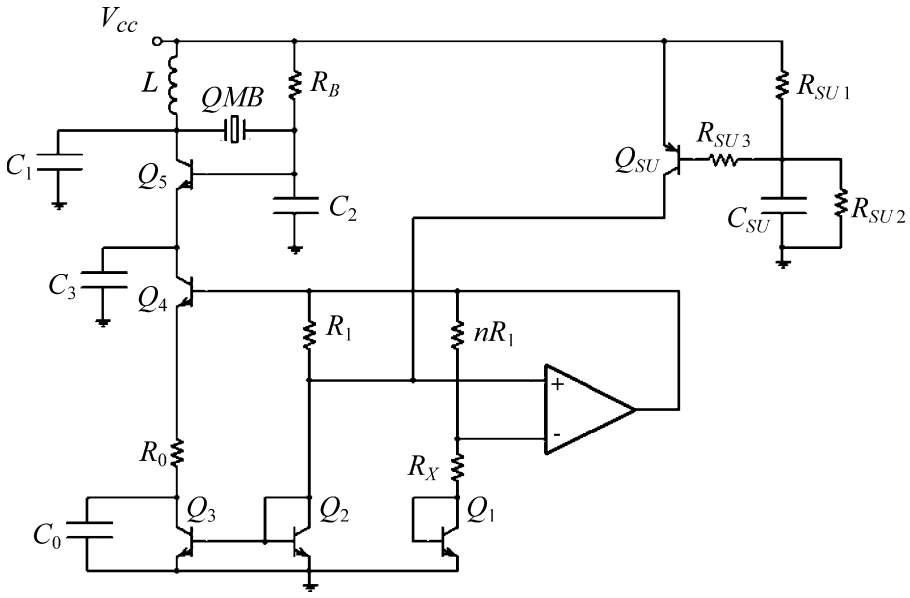

Fig. 69. PTAT oscillator.

biasing strategy easily makes the sensitivity toward supply voltage variations negligible and greatly reduces the sensitivity toward temperature variations [153]. In practice the bandgap circuit generates the PTAT current for biasing Q_5 (which acts as the *v–i* converter of the three points oscillator); the capacitor C_3 dynamically short circuits the emitter of Q_5 to ground and the inductor L dynamically disconnects the collector of Q_4 from ground. Q_{SU}, C_{SU}, R_{SU1}, R_{SU2}, and R_{SU3} implement the start up circuit. For proper operation, the transistors Q_1, Q_2, Q_3 and Q_5 must be well matched and at the same temperature; both these conditions are well satisfied if all those transistors are integrated in the same chip (in this case good matching is possible and the high thermal conductivity of silicon makes sure that all the transistors are at, approximately, the same temperature). If the electronic interface cannot be integrated, a low cost discrete realization is also possible by using a transistor array (i.e. a chip containing a number of well matched transistors). The circuit has been implemented by using a transistor array CA3046. The variation of the oscillating frequency with the voltage supply, for a 20 MHz (i.e. low Q) quartz gave a very low 0.02 ppm/V variation, as shown in Fig. 70; this value is even lower than results (0.05 ppm/V) obtained with automatic gain control and lower frequency (i.e. higher Q) quartzes [150]. As to temperature variations, the CA3046 chip has been heated up by means of a heater in thermal contact with the chip; the temperature of the chip was controlled by measuring the PTAT biasing current; during the measurements, the chip was thermally isolated from the quartz (which was kept at room temperature).

In order to verify the importance of keeping constant the g_m value (i.e. using a PTAT collector current), we have compared the thermal stability of the proposed circuit with that of a standard oscillator that uses a biasing collector current almost independent on temperature (instead of PTAT). Fig. 71 confirms that a significant improvement is obtained if g_m is kept as constant as possible, as it is done in PTAT oscillators.

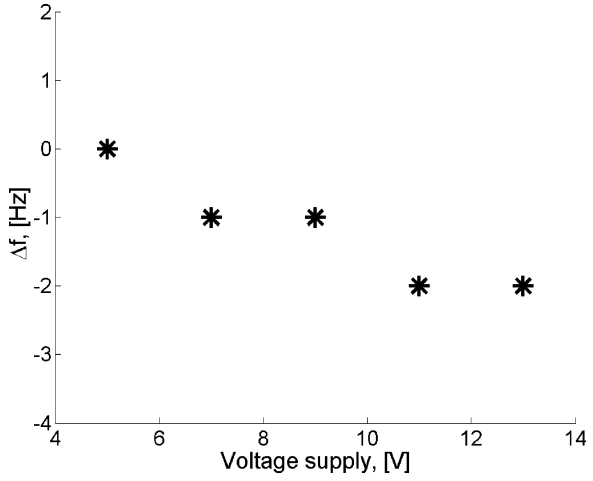

Fig. 70. Frequency variation vs. supply voltage for the PTAT oscillator.

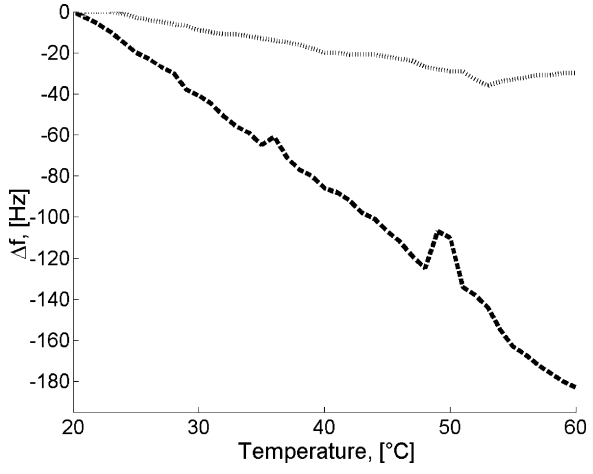

Fig. 71. Measured frequency variation vs. temperature for the PTAT oscillator (dotted line, upper curve) and for a classic oscillator (dashed line, lower curve).

9. Conclusions

In this paper, we have defined smart systems as those systems which are designed by humans and, though non-intelligent, somehow mimic an intelligent behaviour; then, we have shown that sensors, actuators, and electronic interfaces, are at present the necessary and most relevant building blocks for smart systems. A coherent set of definitions which can be applied to sensors, transducers, and electronic interfaces has been given. Depending on the application, electronic interfaces must meet stringent specifications (noise, voltage supply, power consumption, speed, interferences rejection, low cost, reliability, etc.); all these specifications may, in practice, be regarded as design constraints for achieving a predefined accuracy and precision. We have also shown how non-electrical systems may be conveniently modelled by means of equivalent electric circuits; this is an important step for the design of high accuracy and high precision electronic interfaces. Additionally, we have discussed how to identify the most appropriate technology; this choice has a big impact on the design, the performance and the cost of the system, as both the microsystem and the micromodule approach have their merits and their limits with respect to accuracy, precision, reliability, cost, protection against aggressive environment, etc. Moreover, we have shortly reviewed some of the most important techniques for the design and implementation of high accuracy and high precision electronic interfaces, such as feedback, lock in, four wires measurements, etc. Finally, a few case studies have been illustrated.

Acknowledgements

The authors gratefully acknowledge Fabio Lo Castro, Emiliano Zampetti, Simone Pantalei, Giorgio Pennazza, Ubaldo Mastromatteo, Mario Scurati, Fabrizio Mancini, Andrea De Marcellis, Marco Marchesi, Marco Grassi, and Benedetto Vigna for useful technical and scientific discussions.

References

[1] S. Middelhock, S.A. Audet, P. French, Silicon Sensors, Academic Press, London, 2000.
[2] J. Fraden, Handbook of Modern Sensors: Physics, Design and Applications, third ed., Springer, 2003.
[3] S.D. Senturia, Microsystem Design, Kluwer, 2001.
[4] R. Pallàs-Areny, J.G. Webster, Sensors and Signal Conditioning, second ed., Wiley Interscience, 2001.
[5] J.G. Webster (Ed.), Medical Instrumentation: Application and Design, Wiley & Sons, 1998.
[6] A. D'Amico, C. Di Natale, A contribution on some basic definitions of sensors properties, IEEE Sens. J. 1 (3) (October 2001).
[7] G.T.A. Kovacs, N.I. Maluf, K.E. Petersen, Proceedings of the IEEE on Bulk Micromachining of Silicon, August 1998.
[8] J.M. Bustillo, R.T. Howe, R.S. Muller, Proceedings of the IEEE on Surface Micromachining for Microelectromechanical Systems, August 1998.
[9] M.A. Schmidt, Proceedings of the IEEE on Wafer-to-Wafer Bonding for Microstructure Formation, August 1998.
[10] (a) J. Soderkvist, Micromachined gyroscopes, Sens. Actuators A 43 (1994) 65–71;
(b) L.M. Roylance, J.A. Angell, A batch-fabricated silicon accelerometer, IEEE Trans. Electron Devices ED-26 (1979) 1911–1917.
[11] N. Yazdi, F. Ayazi, K. Najafi, Proceedings of the IEEE on Micromachined Inertial Sensors, August 1998, pp. 1640–1659.
[12] A. Gerosa, A. Maniero, A. Neviani, A fully integrated two-channel A/D interface for the acquisition of cardiac signals in implantable pacemakers, IEEE J. Solid-State Circuits 39 (7) (2004) 1083–1093.
[13] B.E. Boser, R.T. Howe, Surface micromachined accelerometers, IEEE J. Solid-State Circuits 31 (3) (1996) 366–375.
[14] M. Lemkin, B.E. Boser, A three-axis micromachined accelerometer with a CMOS position-sense interface and digital offset-trim electronics, IEEE J. Solid-State Circuits 34 (4) (1999) 456–468.
[15] M.S.J. Steyaert, W.M.C. Sansen, A micropower low-noise monolithic instrumentation amplifier for medical purposes, IEEE J. Solid-State Circuits 22 (6) (1987) 1163–1168.
[16] M.A.P. Pertijs, G.C.M. Meijer, J.H. Huijsing, Precision temperature measurement using CMOS substrate pnp transistors, IEEE Sens. J. 4 (3) (2004) 294–300.
[17] E. Wouters, M. De Cooman, R. Puers, A multi-purpose CMOS sensor interface for low-power applications, IEEE J. Solid-State Circuits 29 (8) (1994) 952–956.
[18] A. Bakker, J.H. Huijsing, Micropower CMOS temperature sensor with digital output, IEEE JSSC 31 (7) (1996) 933–937.
[19] M.A.P. Pertijs, K.A.A. Makinwa, J.H. Huijsing, A CMOS smart temperature sensor with a 3 sigma inaccuracy of $\pm 0.1\,^{\circ}C$ from $-55\,^{\circ}C$ to $125\,^{\circ}C$, IEEE JSSC 40 (12) (2005) 2805–2815.
[20] G.C.M. Meijer, A.J.M. Boomkamp, R.J. Duguesnoy, An accurate biomedical temperature transducer with on-chip microcomputer interfacing, IEEE J. Solid-State Circuits 23 (6) (1988) 1405–1410.
[21] M. Ferrari, Cancer nanotechnology: opportunities and challenges, Nature Rev. Cancer 5 (2005) 161–171.
[22] R. Langer, Drug delivery and targeting, Nature 392 (6679) (1998) 5–10.
[23] C. Loo, A. Lin, L. Hirsch, M.H. Lee, J. Barton, N. Halas, J. West, R. Drezek, Nanoshell-enabled phtonics-based imaging and therapy of cancer, Technol. Cancer Res. Treat. 3 (2004) 33–40.
[24] Z.W. Pan, Z.R. Dai, Z.L. Wang, Nanobelts of semiconducting oxides, Science 291 (2001) 1947–1949.
[25] X.Y. Kong, Y. Ding, R.S. Yang, Z.L. Wang, Single-crystal nanorings formed by epitaxial self-coiling of polar-nanobelts, Science 303 (2004) 1348–1351.
[26] P.X. Gao, Y. Ding, W. Mai, W.L. Hughes, C.S. Lao, Z.L. Wang, Conversion of zinc oxide nanobelts into superlattice-structured nanohelices, Science 309 (2005) 1700–1704.
[27] C. Falconi, A. D'Amico, Z.L. Wang, Proceedings of Eurosensors XX on Wireless Nanoactuators and Nanosensors for In-Vivo Biomedical Applications, Goteborg, Sweden, 2006.
[28] X.M.H. Huang, C.A. Zorman, M. Mehregany, M.L. Roukes, Nanodevice motion at microwave frequencies, Nature 421 (2003) 496.
[29] B. Gilbert, Proceedings of the IEEE on Analog at Milepost 2000: A Personal Perspective, vol. 89 (3), March 2001.
[30] P. Malcovati, C. Azeredo Leme, P. O'Leary, F. Maloberti, H. Baltes, Smart sensor interface with A/D conversion and programmable calibration, IEEE J. Solid-State Circuits 29 (8) (1994) 963–966.
[31] V. Peluso, P. Vancorenland, A.M. Marques, M.S.J. Steyaert, W. Sansen, A 900-mV low-power AE A/D converter with 77-dB dynamic range, IEEE J. Solid-State Circuits 33 (12) (1998) 1887–1897.
[32] Y. Libin, M.S.J. Steyaert, W. Sansen, A 1-V 140 μW 88-dB audio sigma-delta modulator in 90-nm CMOS, IEEE J. Solid-State Circuits 39 (11) (2004) 1809–1818.
[33] B.E. Boser, B.A. Wooley, The design of sigma-delta modulation analog-to-digital converters, IEEE J. Solid-State Circuits 23 (6) (1988) 1298–1308.
[34] B.E. Boser, K.P. Karmann, H. Martin, B.A. Wooley, Simulating and testing oversampled analog-to-digital converters, in: IEEE Transactions on Computer-Aided Design of Integrated Circuits and Systems, vol. 7 (6), June 1988, pp. 668–674.
[35] V.P. Petkov, B.E. Boser, A fourth-order Sigma Delta interface for micromachined inertial sensors, IEEE J. Solid-State Circuits 40 (8) (2005) 1602–1609.

[36] G.C.M. Meijer, J.B. Verhoeff, An integrated bandgap reference, IEEE J. Solid-State Circuits 11 (3) (1976) 403–406.
[37] E. Vittoz, O. Neyroud, A low-voltage CMOS bandgap reference, IEEE J. Solid-State Circuits SC-14 (1979) 573–577.
[38] M. Gunawan, G.C.M. Meijer, J. Fonderie, J.H. Huijsing, A curvature-corrected low-voltage bandgap reference, IEEE J. Solid-State Circuits 28 (6) (1993) 667–670.
[39] G.C.M. Meijer, G. Wang, F. Fruett, Temperature sensors and voltage references implemented in CMOS technology, IEEE Sens. J. 1 (3) (2001) 225–234.
[40] P. Malcovati, F. Maloberti, C. Fiocchi, M. M. Pruzzi, Curvature-compensated BiCMOS bandgap with 1-V supply voltage, IEEE J. Solid-State Circuits 36 (7) (2001) 1076–1081.
[41] C. Falconi, J. Huijsing, Proceedings of Eurosensors on Curvature Correction of Bandgap References for Low Cost Integrated Sensors Systems, Prague, Czech Republic, 2003.
[42] C. Falconi, A. D'Amico, C. Di Natale, M. Faccio, Low cost curvature correction of bandgap references for integrated sensors, Sens. Actuators A 117 (2005) 127–136.
[43] G. Massobrio, P. Antognetti, Semiconductor Device Modeling with SPICE, Mc Graw Hill, 1993.
[44] R.S. Muller, T.I. Kamins, Device Electronics for Integrated Circuits, second ed., Wiley, New York, 1986.
[45] S. Sze, Physics of Semiconductor Devices, Wiley and Sons, 1981.
[46] G. Wang, G.C.M. Meijer, The temperature characteristics of bipolar transistors fabricated in CMOS technology, Sens. Actuators 87 (2000) 81–89.
[47] F. Fruett, The piezojunction effect in silicon, its consequences and applications for integrated circuits and sensors, Ph.D. thesis, Delft University of Technology, Delft, The Netherlands, September 2001.
[48] C. Falconi, C. Di Natale, A. D'Amico, J. Huijsing, Proceedings of IEEE Sensors Conference on A Model of Bipolar Transistors for Thermal Sensors Applications, Orlando, Florida, USA, 2002.
[49] S.D. Senturia, Proceedings of the IEEE on CAD Challenges for Microsensors, Microactuators, and Microsystems, August 1998.
[50] N.A. Surplice, R.J. D'Arcy, A critique of the Kelvin method of measuring work functions, J. Phys. E 3 (1970) 477.
[51] P.L. Bergstrom, S.V. Patel, J.W. Schwank, K.D. Wise, A micromachined surface work-function gas sensor for low-pressure oxygen detection, Sens. Actuators B 42 (1997) 195.
[52] A. D'Amico, C. Di Natale, R. Paolesse, A. Mantini, C. Goletti, F. Davide, G. Filosofi, Chemical sensing material characterization by Kelvin probe technique, Sens. Actuators B70 (2000) 254.
[53] L.L. Chu, K. Takahata, P. Selvaganapathy, J.L. Shoher, Y.B. Gianchandani, A micromachined Kelvin Probe for surface potential measurements in microfluidic channels and solid-state applications, Transducers '03, 2D3.1, 384, 2003.
[54] L.L. Chu, K. Takahata, P.R. Selvaganapathy, Y.B. Gianchandani, J.L. Shohet, A micromachined Kelvin probe with integrated actuator for microfluidic and solid-state applications, J. Microelectromech. Syst. 14 (4) (2005).
[55] C. Falconi, F. Lo Castro, L. Fusaro, M. Scoccia, C. Di Natale, Proceedings of AISEM on Automatic System for Work Function Measurement Employing ΣΔ Modulation, 2004.
[56] H. Baltes, CMOS as sensor technology, Sen. Actuators A 37–38 (1993) 51–56.
[57] H. Baltes, D. Moser, E. Lenggenhager, O. Brand, D. Jaeggi, Thermomechanical microtransducers by CMOS and micromachining Micromechanical Sensors, Actuators and Systems, DSC-32, ASME, New York, NY, 1991, pp. 61–75.
[58] H. Baltes, O. Paul, J.G. Korvink, M. Schmeider, J. Bühler, N. Schneeberger, D. Jaeggi, P. Malcovati, M. Hornung, A. Häberli, M. von Arx, F. Mayer, J. Funk, IC MEMS microtransducers, IEDM '96 Technical Digest, 1996, pp. 521–524.
[59] J. Huijsing, Integrated smart sensors, Sens. Actuators A 30 (1992) 167–174.
[60] H. Baltes, O. Brand, CMOS-based microsensors and packaging, Sens. Actuators A 92 (1–3) (2001) 1–9.
[61] A. Baschirotto, P. Malcovati, Technology-driven alternatives for smart sensor interfaces, in: H. Baltes, G. Fedder, J. Korvink (Eds.), Sensors Update, 13, Wiley-VCH, Weinhein, Germany, 2003, pp. 45–81.
[62] G. Palumbo, S. Pennisi, Feedback amplifiers, in: Theory and Design, Kluwer Academic Publishers, 2002.
[63] F. Maloberti, Analog design for CMOS VLSI systems, Kluwer, 2001.
[64] D.A. Johns, K. Martin, Analog Integrated Circuit Design, John Wiley & Sons, 1997.
[65] K.R. Laker, W. Sansen, Design of Analog Integrated Circuits and Systems, McGraw-Hill, New York, 1994.
[66] B. Razavi, Design of Analog CMOS Integrated Circuits, Mc Graw Hill, 2001.
[67] P.R. Gray, P.J. Hurst, S.H. Lewis, R.G. Meyer, Analysis and Design of Analog Integrated Circuits, fourth ed., John Wiley & Sons, 2001, pp. 321.
[68] S. Franco, Design With Operational Amplifiers and Analog Integrated Circuits, McGraw-Hill College, 1988.
[69] J.H. Huijsing, Operational Amplifiers: Theory and Design, Delft University of Technology, Delft, 2000.
[70] R. Gregorian, Introduction to CMOS Op Amps and Comparators, John Wiley & Sons, 1999.
[71] C. Falconi, A. D'Amico, Operational amplifiers, VI EUROSENSORS School on Fundamentals of Sensor Science and Technology, Barcellona, 2005.
[72] V.V. Ivanov, I.M. Filanovsky, Operational Amplifier Speed and Accuracy Improvement: Analog Circuit Design With Structural Methodology, Kluwer, 2004.
[73] C.C. Enz, G.C. Temes, Proceedings of the IEEE on Circuit Techniques for Reducing the Effects of Op-Amp Imperfections: Autozeroing, Correlated Double Sampling, and Chopper Stabilization, vol. 84 (11), 1996, pp. 1584–1614.
[74] A. Bakker, High-Accuracy CMOS smart temperature sensors, Ph.D. thesis, Delft University of Technology, Delft, The Netherlands, April 2000.
[75] A. Bakker, K. Thiele, J.H. Huijsing, A CMOS nested-chopper instrumentation amplifier with 100 nV offset, IEEE JSSC 35 (12) (2000).
[76] S. Kawahito, Proceedings of Eurosensors on Recent Developments in Sensor Interfaces, 2002.
[77] C. Falconi, Principles and circuits for integrated thermal sensors, Ph.D. thesis, University of Tor Vergata, Rome, Italy, December 2001 (chapter 6 (request by email, falconi@eln.uniroma2.it)).
[78] C. Falconi, A. D'Amico, M. Faccio, Proceedings of IEEE ISCAS on Design of Accurate Analog Circuits for Low Voltage Low Power CMOS Systems, vol. 1, 2003, pp. 429–432.
[79] C. Falconi, Proceedings of Eurosensors on High Accuracy Electronic Interfaces for CMOS Microsystems, Rome, Italy, 2004.
[80] C. Falconi, C. Di Natale, A. D'Amico, M. Faccio, Electronic interface for the accurate read-out of resistive sensors in low voltage-low power integrated systems, Sens. Actuators A 117 (2005) 121–126.
[81] C. Enz, Analysis of the low-frequency noise reduction by autozero technique, Electron. Lett. 20 (1984) 959–960.
[82] A. Bakker, K. Thiele, J.H. Huijsing, A CMOS nested-chopper instrumentation amplifier with 100 nV offset, in: Proceedings of the International Solid State Circuit Conference, San Francisco, USA, 2000, pp. 156–157.
[83] R.J. van de Plassche, Dynamic element matching for high accuracy monolithic D/A converters, IEEE JSSC SC-11 (1976).
[84] P.C. De Jong, G.C.M. Meijer, A.H.M. van Roermund, A 300 °C dynamic-feedback instrumentation amplifier, IEEE J. Solid State Circuits 33 (12) (1998) 1999–2009.
[85] P.C. de Jong, G.C.M. Meijer, Absolute voltage amplification using dynamic feedback control, IEEE Trans. Instrum. Meas. 46 (4) (1997) 758–763.
[86] E.A.M. Klumperink, S.L.J. Gierkink, A. Van der Wel, B. Nauta, IEEE JSSC (2000).
[87] C. Falconi, C. Di Natale, A. D'Amico, Proceedings of IEEE ISIE on Low Noise Gain Enhanced Circuits for Low Voltage Low Power CMOS Systems, L'Aquila, Italy, 2002.
[88] C. Falconi, C. Di Natale, A. D'Amico, Proceedings of Eurosensors on Dynamic Op Amp Matching: A New Approach to the Design of Accu-

rate Electronic Interfaces for Low Voltage/Low Power Integrated Sensors Systems, Prague, Czech Republic, 2002.
[89] C. Falconi, M. Faccio, A. D'Amico, C. Di Natale, Proceedings of IEEE ISCAS on High-Accuracy Instrumentation Amplifier for Low Voltage Low Power CMOS Smart Sensors, vol. 3, 2003, pp. 534–537.
[90] C. Falconi, G. Guarino, A. D'Amico, Proceedings of IEEE ISCAS on Op Amp Tuning for High Accuracy Deep Sub-Micron CMOS Analog Circuits, Kobe, Japan, 2005.
[91] C. Falconi, D. Mazzieri, A. D'Amico, V. Stornelli, A. De Marcellis, G. Ferri, Proceedings of Eurosensors on Dynamic Element Matched CC-II for High Accuracy Electronic Interfaces in Deep Sub-Micron CMOS Microsystems, Goteborg, Sweden, 2006.
[92] G. Ferri, P. De Laurentiis, A. D'Amico, C. Di Natale, A low voltage integrated CMOS lock in amplifier prototype for LAPS applications, Sens. Actuators A 92 (2001) 263–272.
[93] M. Tavakoli, R. Sarpeshkar, An offset-canceling low-noise lock-in architecture for capacitive sensing, IEEE J. Solid State Circuits 38 (2) (2003) 244–253.
[94] C. Cantalini, L. Lozzi, M. Passacantando, S. Santucci, The comparative effect of two different annealing temperatures and times on the sensitivity and long-term stability of WO_3 thin films for detecting NO_2, IEEE Sens. J. 3 (2) (2003) 171–179.
[95] I. Hotovy, V. Rehacek, P. Siciliano, S. Capone, L. Spiess, Sensing characteristics of NiO thin films as NO_2 gas sensor, Thin Solid Films 418 (1) (2003) 9–15.
[96] A. Martucci, M. Pasquale, M. Guglielmi, M. Post, J.C. Pivin, Nanostructured silicon oxide nickel oxide sol–gel films with enhanced optical carbon monoxide gas sensitivity, J. Am. Ceram. Soc. 86 (9) (2003) 1638–1640.
[97] L. Fasoli, F. Riedijk, J. Huijsing, A general circuit for resistive bridge sensors with bitstream output, IEEE Trans. Instrum. Meas. 46 (4) (1997).
[98] V. Ferrari, C. Ghidini, D. Marioli, A. Taroni, Oscillator based signal conditioning with improved linearity for resistite sensors, IEEE Trans. Instrum. Meas. 47 (1) (1998) 293–298.
[99] Differential and multiplying digital-to-analog converter applications, Application note AN-19 Analog Devices, http://www.analog.com/.
[100] F. Riedijk, J. Huijsing, An integrated absolute temperature sensor with sigma-delta A-D conversion, Sens. Actuators A 34 (1992) 9–16.
[101] V. Ferrari, C. Ghidini, D. Marioli, A. Taroni, Proceedings of the 16th IMTC on Oscillator Based Interface for Measurand-Plus-Temperature Readout From Resistive Bridge Sensors, vol. 2, 24–26 May 1999, pp. 1233–1238.
[102] J.H. Huijsing, G.A. Van Rossum, M. Van der Lee, Two-wire bridge-to-frequency converter, IEEE JSSC 22 (3) (1987) 343–349.
[103] G.J.A. van Dijk, J.H. Huijsing, Bridge-output-to-frequency converter for smart thermal air-flow sensors, IEEE Trans. Instrum. Meas. 44 (4) (1995) 881–886.
[104] A. Morgenshtein, L. Sudakov-Boreysha, U. Dinnar, C.G. Jakobson, Y. Nemirovsky, Wheatstone bridge readout interface for IFET-REFET applications, Sens. Actuators B 98 (2004) 18–27.
[105] A. D'Amico, C. Di Natale, G. Ferri, A ±0.6 V-supply CMOS topology to improve Wheatstone bridge performance, IV AISEM (Associazione Italiana Sensori e Microsistemi) Conference—AISEM 99, Roma, 3–5 February 1999, pp.403–407, available after request to ferri@ing.univaq.it.
[106] A. Sedra, G.W. Roberts, F. Gohh, IEE Proceedings on The Current Conveyor: History, Progress and New Results, vol. 137 (2), pp. 78–87, April 1990 (Pt. G).
[107] G. Ferri, N.C. Guerrini, Low Voltage Low Power Current Conveyors, Kluwer Academic Publisher, Boston, July 2003.
[108] G. Ferri, V. Stornelli, M. Fragnoli, An integrated improved CCII topology for resistive sensor application, Analog Integrated Circuits Signal Processing 49 (3) (2006).
[109] C. Cantalini, G. Ferri, N. Guerrini, S. Santucci, A low-voltage low-power current-mode gas sensor integrated interface, in: International Conference on Microelectronics (ICM) 2004, Monastir, Tunisia, 2004.
[110] G. Ferri, P. De Laurentiis, Proceedings ISCAS 2000 on A Low Voltage CMOS Phase Shifter As A Resistive Sensor Transducer, vol.2, Genova, 28–31 May 2000, pp. 605–608, ISBN 0-7803-5485-0.
[111] G. Ferri, V. Stornelli, A. De Marcellis, A. Flammini, A. Depari, Novel CMOS integrable wide-range resistive sensor interface, in: 11th International Meeting on Chemical Sensors, IMCS 2006, Brescia, 16–19 July 2006.
[112] A. Flammini, D. Marioli, A. Taroni, A low-cost interface to high-value resistive sensors varying over a wide range, IEEE Trans. Instrum. Meas. 53 (4) (2004).
[113] H.T. Chueh, J.V. Hatfield, A real-time data acquisition system for a hand-held electronic nose, Sens. Actuators B 83 (2002) 262–269.
[114] G. Sberveglieri, Recent developments in semiconducting thin-film gas sensors, Sens. Actuators B 23 (1995) 103–109.
[115] S. Capone, P. Siciliano, Gas sensors from nanostructured metal oxides, Encyclopedia Nanosci. Nanotechnol. 3 (2004) 769–804.
[116] A. Flammini, D. Marioli, A. Taroni, A low-cost interface to high value resistive sensors varying over a wide range, in: Proceedings of IEEE Instrumentation and Measurement Technology Conference, Veil, USA, 2003, pp. 726–731.
[117] D. Barrettino, M. Graf, W.H. Song, K. Kirstein, A. Hierlemann, Hotplate-based monolithic CMOS microsystems for gas detection and material characterization for operating temperatures up to 500 °C, IEEE J. Solid State Circuits 39 (2004) 1202–1207.
[118] M. Grassi, P. Malcovati, A. Baschirotto, A 0.1% accuracy 100 Ω–20 MΩ dynamic range integrated gas sensor interface circuit with 13 + 4 bit digital output, in: Proceedings of IEEE European Solid-State Circuits Conference, Grenoble, France, 2005, pp. 351–354.
[119] M. Grassi, P. Malcovati, A. Baschirotto, A high-precision wide-range front-end for resistive gas sensors arrays, Sens. Actuators B 111–112 (2005) 281–285.
[120] P. Malcovati, M. Grassi, F. Borghetti, V. Ferragina, A. Baschirotto, Design and characterization of a 5-decade range integrated resistive gas sensor interface with 13-bit A/D converter, in: Proceedings of IEEE International Conference on Sensors, Irvine, USA, 2005, pp. 472–475.
[121] H.J. Verhoeven, Smart thermal flow sensors, Ph.D. thesis, Delft University of Technology, Delft, 1995.
[122] B.W. van Oudheusden, in: G.C.M. Meijer, A.W. van Herwaarden (Eds.), Thermal Flow Sensors, Institute of Physics Publishing Bristol and Philadelphia, London, 1994.
[123] F. Lo Castro, C. Falconi, A. D'Amico, C. Di Natale, U. Mastromatteo, M. Scurati, G. Barlocchi, P. Corona, M. Cattaneo, F. Villa, Proceedings of Eurosensors on Temperature Control System for Lab On Chip Applications, Rome, Italy, 2004.
[124] C. Falconi, E. Zampetti, S. Pantalei, E. Martinelli, C. Di Natale, A. D'Amico, V. Stornelli, G. Ferri, Proceedings of IEEE ISCAS on Temperature and Flow Velocity Control for Quartz Crystal Microbalances, Kos, Greece, 2006.
[125] C. Falconi, A. Mauri, M. Fratini, A. D'Amico, V. Stornelli, A. De Marcellis, G. Ferri, Proceedings of Eurosensors on Thermal ΣΔ Modulation for CMOS Microsystems Temperature Control, Goteborg, Sweden, 2006.
[126] C.H. Mastrangelo, M.A. Burns, D.T. Burke, Proceedings of the IEEE on Microfabricated Devices for Genetic Diagnostics, vol. 86 (8), August 1998, pp. 1769–1787.
[127] S.O. Choi, S. Kawahito, Y. Matsumoto, M. Ishida, Y. Tadokoro, An integrated micro fluxgate magnetic sensor, Sens. Actuators A 55 (1996) 121–126.
[128] P.M. Drljaca, P. Kejik, F. Vincent, D. Piguet, R.S. Popovic, Low-power 2-D fully integrated CMOS fluxgate magnetometer, IEEE Sens. J. (2005) 1–7.
[129] A. Baschirotto, E. Dallago, P. Malcovati, M. Marchesi, G. Venchi, Precise vector-2D magnetic field sensor system for electronic compass, in: Proceedings of IEEE Sensors, Wien, Austria, 2004, pp. 1028–1031.
[130] P. Ripka, S.O. Choi, A. Tipek, S. Kawahito, M. Ishida, Pulse excitation of micro-fluxgate sensors, IEEE Trans. Magn. 37 (2001) 1998–2000.
[131] A. Baschirotto, F. Borghetti, E. Dallago, P. Malcovati, M. Marchesi, E. Melissano, P. Siciliano, G. Venchi, Fluxgate magnetic sensor and front-end circuitry in a micro-integrated system, in: Proceedings of Eurosensors, Barcellona Spain, 2005, p. WPb42.

[132] A. Baschirotto, E. Dallago, P. Malcovati, M. Marchesi, E. Melissano, P. Siciliano, G. Venchi, An integrated micro-fluxgate magnetic sensor with sputtered ferromagnetic core, in: Proceedings of IEEE Instrumentation and Measurement Technology Conference, Sorrento, Italy, 2005, pp. 2045–2049.
[133] A. Baschirotto, F. Borghetti, E. Dallago, P. Malcovati, M. Marchesi, G. Venchi, A CMOS front-end circuit for integrated fluxgate magnetic sensors, in: Proceedings of IEEE International Symposium on Circuits and Systems, Kos, Greece, 2006, pp. 4403–4406.
[134] G. Spinola, S. Zerbini, B. Vigna, Silicon integrated gyroscope and accelerometers, Multifunction sensors for structural health monitoring in aerospace structures workshop, Capua, Italy, 2001.
[135] J.H. Smith, S. Montague, J.J. Sniegowski, J.R. Murray, P.J. McWhorter, Proceedings of the IEDM on Embedded Micromechanical Devices for the Monolithic Integration of MEMS with CMOS, 1995, pp. 609–612.
[136] T. Smith, O. Nys, M. Chevroulet, Y. DeCoulon, M. Degrauwe, A 15 b electromechanical Sigma-Delta converter for acceleration measurements, ISSCC Dig. Tech Papers, February 1994, pp. 160–161.
[137] L.J. Ristic, R. Gutteridge, B. Dunn, D. Mietus, P. Bennett, Proceedings of the IEEE Solid-State Sensor and Actuator Workshop on Surface Micromachined Polysilicon Accelerometer, June 1992, pp. 118–121.
[138] A. Gola, N. Bagnalasta, P. Bendiscioli, E. Chiesa, S. Delbò, E. Lasalandra, F. Pasolini, M. Tronconi, T. Ungaretti, A. Baschirotto, A MEMS-based rotational accelerometer for HDD applications with 2.5 rad/s^2 resolution and digital output, in: Proceedings of European Solid-State Circuits Conference, 2001, pp. 336–339.
[139] P. Hauptmann, Resonant sensors and applications, Sens. Actuators A 25–27 (1991) 371–377.
[140] R. Lucklum, B. Henning, P. Hauptmann, K.D. Schierbaum, S. Vaihinger, W. Gopel, Quartz microbalance sensors for gas detection, Sens. Actuators A 25–27 (1991) 705–710.
[141] T. Schenider, D. Richter, S. Doerner, H. Fritze, P. Hauptmann, Proceedings of Eurosensors XVIII on Novel Impedance Interface for Resonant High-Temperature Gas Sensors, Rome, 2004, pp. 103–104.
[142] R. Borngraber, J. Schroder, R. Lucklum, P. Hauptmann, Is an oscillator-based measurement adequate in a liquid environment? IEEE Trans. Ultrason. Ferroelectr. Freq. Control 49 (9) (2002) 1254–1259.
[143] J. Rabe, S. Buttgenbach, J. Schroder, P. Hauptmann, Monolithic miniaturized quartz microbalance array and its application to chemical sensor systems for liquids, IEEE Sens. J. 3 (4) (2003) 361–368.
[144] J. Auge, P. Hauptmann, J. Hartmann, S. Rosler, R. Lucklum, New design for QCM sensors in liquids, Sens. Actuators B 24–25 (1995) 43–48.
[145] J. Auge, P. Hauptmann, F. Eichelbaum, S. Rosler, Quartz crystal microbalance sensor in liquids, Sens. Actuators B 18–19 (1994) 518–522.
[146] F. Eichelbaum, R. Borngraber, J. Schroder, R. Lucklum, Interface circuits for quartz crystal microbalance sensors, Rev. Scientific Instrum. 70 (5) (1999) 2537–2545.
[147] J. Schroder, R. Borngraber, F. Eichelbaum, P. Hauptmann, Advanced interface electronics and methods for QCM, Sens. Actuators A 97–98 (2002) 543–547.
[148] B. Zimmermann, R. Lucklum, P. Hauptmann, J. Rabe, S. Buttgenbach, Electrical characterisation of high frequency thickness shear mode resonators by impedance analysis, Sens. Actuators B 76 (2001) 47–57.
[149] R. Lucklum, C. Behling, P. Hauptmann, Gravimetric and non-gravimetric chemical quartz crystal resonators, Sens. Actuators B 65 (2000) 277–283.
[150] E.A. Vittoz, M.G.R. Degrauwe, S. Bitz, High-performance crystal oscillator circuits: theory and application, IEEE J. Solid State Circuits 23 (3) (1988) 774–783.
[151] R.A. Bianchi, J.M. Karam, B. Courtois, Analog ALC crystal oscillators for high-temperature applications, IEEE Trans. Solid-State Circuits 35 (1) (2000) 2–14.
[152] C. Falconi, E. Zampetti, A. Massari, C. Di Natale, A. D'Amico, Proceedings of Eurosensors on High Precision Oscillator for QMB Sensors, Rome, Italy, 2004.
[153] C. Falconi, A. Massari, A. D'Amico, PTAT oscillators for low Q resonating sensors, Sens. Actuators, B: Chem. 113 (1) (2006) 120–126.

Biographies

Christian Falconi was born in Rome, Italy, 1973. He received the MSc (cum laude) and the PhD degrees in electronic engineering from the University of Tor Vergata, Rome, Italy, in, respectively, 1998 and 2001; as a part of his PhD program he visited the University of Linköping (1 month), and TU Delft (7 months). In 2002 he has supervised the design of the electronic interface for the ST-Microelectronics DNA chip. Since 2002 Christian Falconi is Assistant Professor at the Department of Electronic Engineering, University of Tor Vergata, where he teaches Low Voltage Analog Electronics and Fundamental of Electronics. Since 2003 he has been visiting the Georgia Institute of Technology (9 months). He authored or co-authored more than 30 papers on international journals and conference proceedings. His research interests include electronic devices, analog circuits, electronic interfaces, sensors, microsystems, and nanosystems.

Eugenio Martinelli has a post-doc position at the Department of Electronic Engineering of the University of Rome Tor Vergata. His research activities are concerned with the development of artificial sensorial systems (olfaction and taste) and their applications, sensor interfaces and data processing. He authored more than 50 papers on international journals and conference proceedings. He has been responsible of two experiments during the Eneide Space Mission on the International Space Station (April, 2005).

Corrado Di Natale is an associate professor at the Faculty of Engineering of the University of Rome Tor Vergata where he teaches courses on Sensors and Detectors. His research activities are concerned with the development of chemical and bio-sensors, artificial sensory systems (olfaction and taste) and their applications, and the study of the optical and electronic properties of organic and molecular materials. Corrado Di Natale authored more than 400 papers on international journals and conference proceedings. In September 2006 he received the Eurosensors Fellow Award for his contributions in the field of artificial sensory systems. He chaired the 9th International Symposium on olfaction and electronic nose (Rome, 2002) and Eurosensors XVIII (Rome, 2004) and was member of the organizing committee of several international conferences in sensors. He serves as component of the steering committee of the Eurosensors conferences series and as associate editor of IEEE Sensors Journal. He edited several proceedings volumes, and is a regular referee for many journals in the field.

Arnaldo D'Amico received the Laurea degree in physics and electronic engineering from the University La Sapienza, Rome, Italy. For several years, he has been with the National Research Council (CNR) leading the Semiconductors Laboratory at the Solid State Electronic Institute, Rome. In 1988, he was appointed Full Professor of electronics at the University of L'Aquila, and, since 1990, he has been with the University of Rome Tor Vergata where he leads the Sensors and Microsystems Group and is Full Professor of electronics, Faculty of Engineering. He teaches courses on electronic devices, microsystems, and sensors. Currently, his main research activities are concerned with the development of physical and chemical sensors, low voltage electronics, noise, and advanced electronic devices. He is author of more than 450 papers in international journals and conference proceedings. He has been Chairman of several conferences on sensors, electronics, and noise and a member of the editorial board of the journals Sensors and Actuators A (physical) and Sensors and Actuators B (chemical). He served as Chairman of the Steering Committee of the Eurosensors conference series from 1999 to 2004. At the national level, he is Chairman of the National Society of Sensors and Microsystems (AISEM) and Director of the Institute of Acoustics "O. M. Corbino" of the National Research Council (CNR).

Franco Maloberti received the Laurea degree in Physics (Summa cum Laude) from the University of Parma, Parma Italy, in 1968 and the Dr. Honoris Causa degree in electronics from the Instituto Nacional de Astrofisica, Optica y Electronica (Inaoe), Puebla, Mexico in 1996. He was a Visiting Professor at ETH-PEL, Zurich in 1993 and at EPFL-LEG, Lausanne in 2004. He was Professor of Microelectronics and Head of the Micro Integrated Systems Group University of Pavia, Italy and the TI/J.Kilby Analog Engineering Chair Professor at the Texas A&M University. He was also the Distinguished Microelectronic Chair Professor at University of Texas at Dallas. Currently he is Professor at the University of Pavia, Italy. His professional expertise is in the design, analysis and characterization of integrated circuits and analogue digital applications, mainly in the areas of switched capacitor circuits, data converters, interfaces for telecommunication and sensor systems, and CAD for analogue and mixed A-D design. He has written more than 300 published papers, three books and holds 17 patents. He was in 1992 recipient of the XII Pedriali Prize for his technical and scientific contributions to national industrial production. He was co-recipient of the 1996 Institute of Electrical Engineers (U.K.) Fleming Premium for the paper "CMOS Triode Transistor Transconductor for high-frequency continuous time filters." He has been responsible at both technical and management levels for many research programs including ten ESPRIT projects and has served the European Commission as ESPRIT Projects' Evaluator, Reviewer and as European Union expert in many European Initiatives. He served the Academy of Finland on the assessment of electronic research in Academic institutions and on the research programs' evaluations. He served the National Research Council of Portugal on a Board for the research activity assessment of Portuguese Universities. Dr. Maloberti was Vice-President, Region 8, of the IEEE Circuit and Systems Society from 1995 to 1997 and an Associate Editor of IEEE-Transaction on Circuit and System-II in 1998. He received the 1999 IEEE CAS Society Meritorious Service Award, the 2000 CAS Society Golden Jubilee Medal, and the IEEE Millenium Medal. He was the President of the IEEE Sensor Council (2002–2003). He is a member of the BoG of the IEEE-CAS Society (2003–2005). He is an Associate Editor of the IEEE-TCAS II, member of the Editorial Board of Analog Integrated Circuits and Signal Processing, and Fellow of IEEE.

Piero Malcovati was born in Milano, Italy in 1968. He received the "Laurea" degree (Summa cum Laude) in electronic engineering from University of Pavia, Italy in 1991. In 1992 he joined the Physical Electronics Laboratory (PEL) at the Federal Institute of Technology in Zurich (ETH Zurich), Switzerland, as a PhD candidate. He received the PhD degree in Electrical Engineering from ETH Zurich in 1996. From 1996 to 2001 he has been Assistant Professor at the Department of Electrical Engineering of the University of Pavia. From 2002 Piero Malcovati is Associate Professor of Electrical Measurements in the same institution. His research activities are focused on microsensor interface circuits and high performance data converters. He authored and co-authored more than 20 papers in International Journals, more than 50 presentations at International Conferences (with published proceedings), 4 book chapters, and 3 industrial patents. He was guest editor for the Journal of Analog Integrated Circuits and Signal Processing for the special issue on IEEE ICECS 1999. He served as Special Session Chairman for the IEEE ICECS 2001 Conference, as Secretary of the Technical Program Committee for the ESSCIRC 2002 Conference and as Technical Program Chairman of the IEEE PRIME 2006 Conference. He was and still is member of the Scientific Committees for several International Conferences, including ESSCIRC, DATE and PRIME. He is associate editor of the Journal of Circuits, Systems, and Computers. He is an IEEE senior member.

Andrea Baschirotto was born in Legnago (VR), Italy in 1965. He graduated in electronic engineering (summa cum laude) from the University of Pavia in 1989. In 1994, he received the PhD degree in electronic engineering from the University of Pavia. In 1994, he joined the Department of Electronics, University of Pavia, as a Researcher (Assistant Professor). In 1998, he joined the Department of Innovation Engineering, University of Lecce, Italy, as an Associate Professor. Since 1989, he has collaborated with several companies on the design of mixed signals ASICs. He participates to several research collaborations, also funded by National and Europen projects. He is now the Coordinator of a National project for the design of large-dynamic range gas sensors. His main research interests are in the design of mixed analog/digital integrated circuits, in particular for low-power and/or high-speed signal processing. He has authored or co-authored more than 160 papers in international journals and presentations at international conferences, 6 book chapters, and holds 25 industrial patents. In addition, he has co-authored more than 120 papers within research collaborations on high-energy physics experiments. Prof. Baschirotto was Associate Editor of IEEE Trans. Circuits Syst.—Part II for the period 2000–2003, and he is now serving IEEE Trans. Circuits Syst.—Part I as an associate editor. He has been the Technical Program Committee Chairman for ESSCIRC 2002 and he was the guest editor for the IEEE J. Solid-State Circ. for ESSCIRC 2003. He is the member of the Technical Program Committee of several conferences (ISSCC, ESSCIRC, DATE, etc.). He is IEEE Senior member.

Vincenzo Stornelli was born in Avezzano (AQ), Italy. He received the electronic engineering degree (cum laude) in July 2004. In October 2004 he joined the Department of Electronic Engineering, University of L'Aquila, where he is actually involved with problems concerning physics-based simulation, CAD modeling characterization and design analysis of active microwave components, circuits, and subsystems project and design of integrated circuits for RF and sensor applications. His research interests also include several topics in computational electromagnetic, including microwave antennas analysis for outdoor UWB applications. He regularly teaches courses of the European Computer patent and has collaborations with national corporations such as Thales Italia.

Giuseppe Ferri was born in L'Aquila, Italy, in 1965. He received his "laurea" degree in 1988 in electronic engineering in the University of L'Aquila. In 1991 he became assistant professor in the area of electronics at the same university. Since 2001 he has been an Associate Professor of electronics at the University of L'Aquila. His main scientific interests are: low voltage low power analog design for portable applications (sensors, biomedicals, etc.), current-mode techniques and circuit theory. In this areas he is author and co-author of 5 books and of 75 papers published on scientific Journals and more than 120 talks at national and international conferences. He is a senior member of IEEE.